EXPERIMENTAL FEASIBILITY STUDY OF RADIAL INJECTION COOLING OF THREE-PAD RADIAL AIR FOIL BEARINGS

by

SUMAN K SHRESTHA

Presented to the Faculty of the Graduate School of
The University of Texas at Arlington in Partial Fulfillment
of the requirements
for the degree of

MASTER OF SCIENCE IN MECHANICAL ENGINEERING

THE UNIVERSITY OF TEXAS AT ARLINGTON
August 2012

ACKNOWLEDGEMENTS

I would like to thank my committee chair, Dr. Daejong Kim for his guidance, and support throughout the course of research. I would also like to thank Dr. Kent Lawrence and Dr. Bo Wang for serving as committee members. I would like to thank my colleagues at Microturbomachinery and Energy Systems Laboratory for their help, support and advices.

I would like to thank Kermit and Sam from machine shop for their valuable advices and willingness to help throughout my research.

I would also like to acknowledge the financial support provided to me by the Dr. Daejong Kim and Dr. Roger Goolsby Endowment Scholarship from the Department of Mechanical and Aerospace, The University of Texas at Arlington.

And above all I would like to thank my family and friends whose support and encouragements kept me going and being successful.

May 14, 2012

ABSTRACT

EXPERIMENTAL FEASIBILITY STUDY OF RADIAL INJECTION COOLING OF THREE-PAD RADIAL AIR FOIL BEARINGS

Suman K Shrestha, M.S.

The University of Texas at Arlington, 2012

Supervising Professor Daejong Kim

Air foil bearings use ambient air as a lubricant allowing environment-friendly operation. When they are designed, installed, and operated properly, air foil bearings are very cost effective and reliable solution to oil-free turbomachinery. Because air is used as a lubricant, there are no mechanical contacts between the rotor and bearings and when the rotor is lifted off the bearing, near frictionless quiet operation is possible. However, due to the high speed operation, thermal management is one of the very important design factors to consider. Most widely accepted practice of the cooling method is axial cooling, which uses cooling air passing through heat exchange channels formed underneath the bearing pad. Advantage is no hardware modification to implement the axial cooling because elastic foundation structure of foil bearing serves as a heat exchange channels. Disadvantage is axial temperature gradient on the journal shaft and bearing.

This work presents the experimental feasibility study of alternative cooling method using radial injection of cooling air directly on the rotor shaft. The injection speeds, number of nozzles, location of nozzles, total air flow rate are important factors determining the effectiveness of the radial injection cooling method. Effectiveness of the radial injection cooling was compared with traditional axial cooling method.

A previously constructed test rig was modified to accommodate a new motor with higher torque and radial injection cooling. The radial injection cooling utilizes the direct air injection to

the inlet region of air film from three locations at 120^{o} from one another with each location having three axially separated holes. In axial cooling, a certain axial pressure gradient is applied across the bearing to induce axial cooling air through bump foil channels. For the comparison of the two methods, the same amount of cooling air flow rate was used for both axial cooling and radial injection. Cooling air flow rate was referenced to the rotor surface speed for radial injection cooling. The mass flow rates for the radial injection were 0.032, 0.0432, 0.054 and 0.068 Kg/min, which result in average injection speed of 150, 200, 250 and 300% of rotor surface speed. Several thermocouples were attached at various circumferential directions of the bearing sleeve, two plenums, bearing holder and ball bearing housings to collect the temperature data of the bearing at 30krpm under 10lb of load.

Both axial cooling and radial injection are effective cooling mechanism and effectiveness of both cooling methods is directly proportional to the total mass flow rates. However, axial cooling is slightly more efficient in controlling the average temperature of the bearing sleeve, but results in higher thermal gradient of the shaft along the axial direction and also higher thermal gradient of the bearing sleeve along the circumferential direction compared to the radial injection cooling. The smaller thermal gradient of the radial injection cooling is due to the direct cooling effect of the shaft by impinging jets. While the axial cooling has an effect on only the bearing, the radial injection has a cooling effect on both the bearing sleeve and shaft. It is considered the radial injection cooling needs to be further optimized in terms of number of injection holes and their locations.

TABLE OF CONTENTS

LIST OF ILLUSTRATIONS

Figure Page

LIST OF TABLES

Table Page

CHAPTER 1

INTRODUCTION

Currently, there is high demand of the fluid (oil/gas) film bearings in turbo machinery industry. Oil lubricated bearings are widely used in the industries. However some researchers in small high speed turbomachinery have been exploring better ways to replace these oil lubricated bearings because of their limitations such as thermal degradation of oil over time, complicated oil lubrication systems and their maintaince. Another type of fluid film bearing is Air (gas) Foil Bearing (AFB) which operates on air as lubricant and can overcome some issues of oil lubricated bearing; use of AFB eliminates need for complicated oil lubrication system reducing need of costly equipments and maintenance, it can run at high speed in extreme temperature without the risk of thermal degradation of the lubricant. Also load carrying capacity of these bearings increase with the speed which is ideal for the small turbo machinery system with very high speeds [1]. The applications of the AFB currently include cryogenic turbo expander, micro turbines, air cycle machines, small aero-propulsion engines, fuel cells and so on.

1.1 Air Foil Bearings

AFB consists of a hollow (cylindrical) bearing surface which sits around the shaft. Inner surface of the bearing can be circular or tailored to have certain amount of preload which can accommodate the higher speed, small imbalances and rotor-bearing misalignment. Namely the basic component of bearing are sleeve, smooth sheet metal called top foil and corrugated support structure called bump foil over which the top foil resides. Figure 1-1 shows the configuration of the typical single pad AFB with a top foil, bump foil and bearing sleeve. Due to high friction power loss during start/stop cycles, the top foil is usually coated with solid lubricant such as Teflon. PS 300, another solid lubricant for journal shaft developed by NASA

researchers [put reference here] is claimed to have better wear protection during start/stops cycle at very high temperature up to 700^{o}C. The bump foil provides stiffness and damping properties to the bearing which can be controlled by tailoring the bump height, materials and the overall geometry. Typically the nickel-based super alloy such as Inconel (Inconel is a registered trademark of Special Metals Corporation that refers to a family of austenitic nickel-chromium-based superalloys) is used for the foils due to its excellent mechanical properties at high temperature. It is important to note that the direction of rotation of AFB is from trailing edge to leading edge as shown in the Figure 1-1 below.

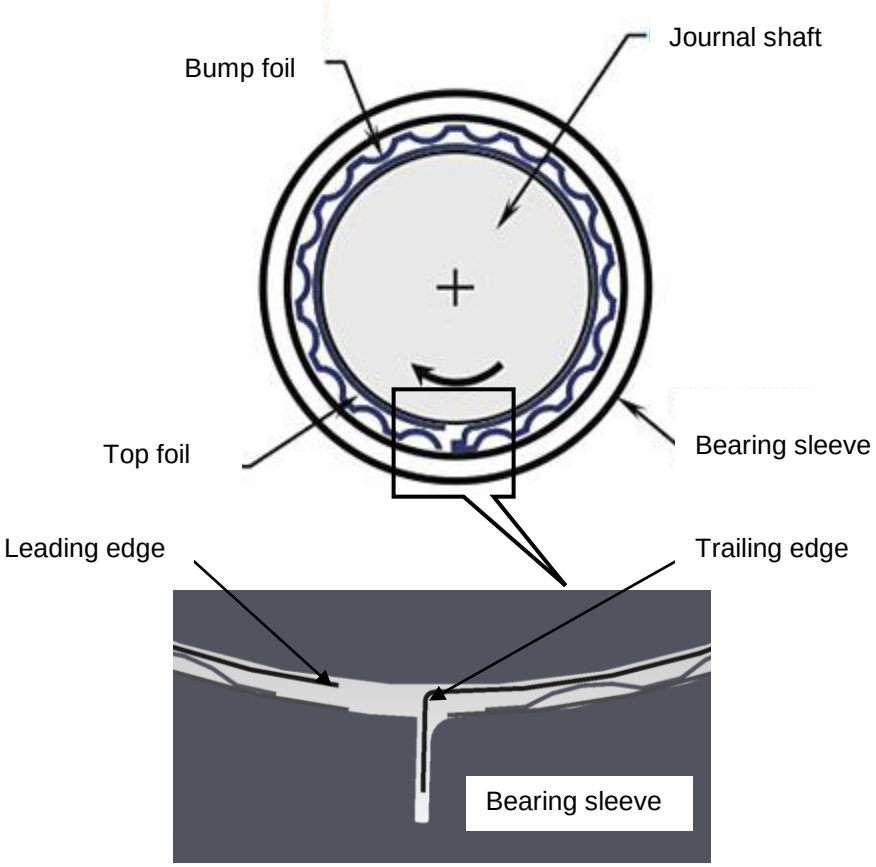

Figure 1-1 Typical single pad AFB configuration

1.2 Operating Principle of Air Foil Bearings

When the shaft is set to motion, hydrodynamic pressure is built up between the rotating shafts and bearing surface .The pressure generated is via two mechanisms: wedge effect and squeeze film effect. When journal shaft is rotating and bearing is stationary the converging surfaces builds up the pressure, which is known as the wedge effect. Similarly, squeezing of the air molecules in the clearance area causes them to escape to ambient air. However, these molecules' motion is resisted by the surrounding molecules, building up the positive pressure. Combination of these two effects gives the bearings enough hydrodynamic pressure needed to lift the shaft and maintain the clearance with the stationary bearing surface. Hence at the steady state, there is no contact between the shaft and the bearing. The presence of corrugated bump foil gives the bearing necessary stiffness and damping which can accommodate external shocks, rotor misalignment and rotor run outs.

Similar operating principle is applied to hydrodynamically preloaded three pad AFB (see Figure 1-2), which is consisted of three top foils supported by independent bump foils. The three-pad AFB has many attractive features such as higher rotor-bearing stability and lower start/stop friction compared to the circular single pad bearings. Set bore clearance (Cs) is the actual minimum clearance in the bearing, and amount of hydrodynamic preload (Rp) corresponds to the distance between the bearing center and individual pad center.

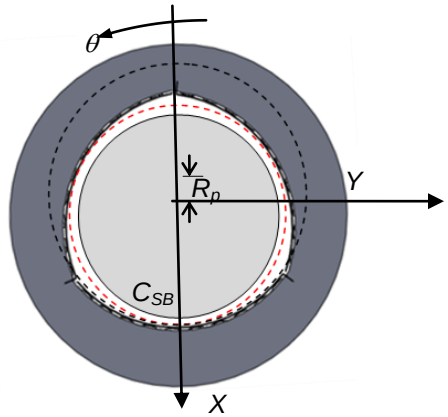

Figure 1-2 Three-pad AFB with preload (Rp), set bore clearance(Cs) and pad configuration

1.3 Disadvantages of Air Foil Bearings

Even though AFBs have many favorable features over traditional oil lubricated bearings systems, it has some issues involving thermal management, instability due to cross coupled stiffness, start/stop frictions, and load capacity. Thermal issue of AFB generally occurs due to the viscous shearing of the air film in the clearance area (area between journal shaft and top foil). Also at higher speed, the centrifugal growth and thermal expansion of journal shaft results in reduction of the air film, and eventually thermal runaway. The thermal runaway puts the limit on highest rotor speed as well as the load capacity of AFB.

Since air has low heat capacity, small amount of heat transferred from outside can increase the bearing temperature significantly in comparison to oil. Also AFB has spatially varying stiffness and air film thickness which can trap the air in the clearance area. Viscous heating of this trapped air leads to the formation of localized thermal gradients resulting distortion of top foil and eventually failure of the bearing systems [5].

CHAPTER 2

LITERATURE REVIEW

Radil et al [1] evaluated the thermal behavior of air foil bearings with three different cooling techniques. The first and second methods were cooling of the journal shaft via direct and indirect impingement of cooling air to the inner diameter surface of the hollow shaft as described in Figure 2-1. The direct cooling techniques uses air injected toward the inner diameter surface of the journal shaft. Indirect cooling technique uses axial cooling air through a hollow shaft. The third method is using axial cooling air flow through the bump foil channels. Among all the three methods, the axial cooling through the bump foil channels was proved to be the most effective to reduce the bearing internal temperature.

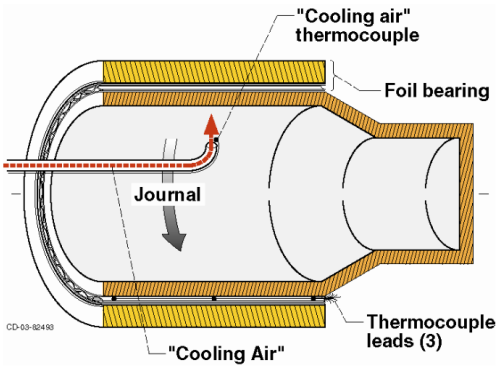

(a)

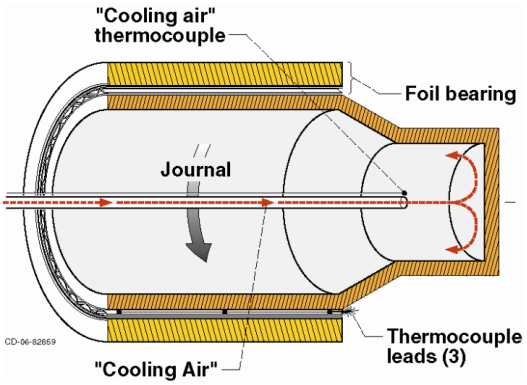

(b)

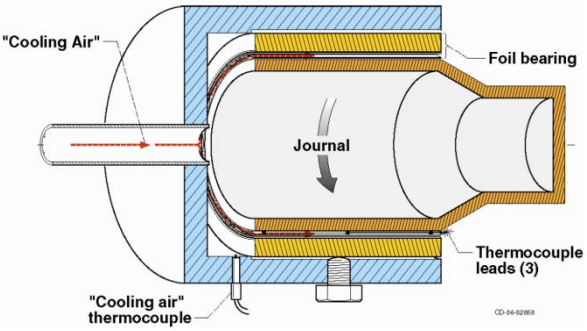

(c)

Figure 2-1 Three different cooling methods (a) Direct cooling (b) Indirect cooling (c) Axial cooling adopted from [1]

Radil and Batcho [2] conducted an experiment to evaluate alternative cooling method to a radial foil bearing with single top foil. The idea behind their work was to investigate whether injection of cooling air to the leading edge region, where top foil is discontinuous (as shown in Figure 1-1), could reduce the bearing bulk temperature. The original intention of their approach was to inject cooling air directly into the leading edge of the top foil. However, as shown in their experimental set up (see Figure 2-2), location of the hole for air impingement was space between the leading and trailing edge of the top foil. The authors of this paper clearly states that no attempts were made for the optimization of hole size, shape, or orientation. The experiment was conducted at two different speeds, 20krpm and 40 krpm, with load of 222N and cooling air flow rate of 0.017 Kg/min and 0.051 Kg/min.Higher flow rate showed better cooling effectiveness as expected. Also the authors conducted further investigation to test the effectiveness of the cooling technique at higher speeds but quickly realized the need of higher air flow rate up to 0.068Kg/min to achieve thermal stability. They conclude that injection of air directly to the shaft is not as effective as traditional axial cooling method. However, maximum air injection speed is around 100m/s, which is not considered high enough to break the thermal boundary layer attached to the shaft, as will be demonstrated later in the current thesis.

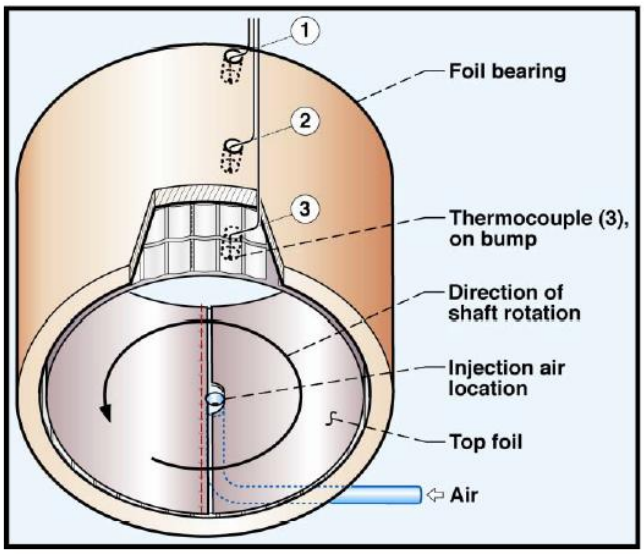

(a)

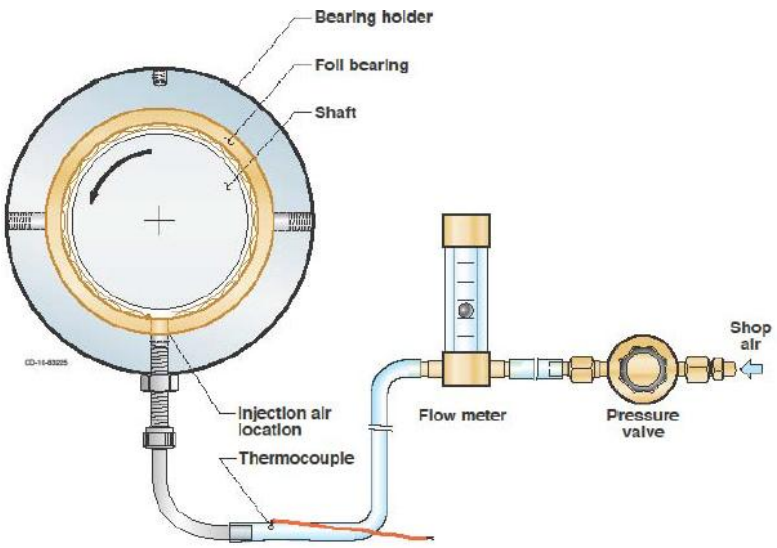

(b)

Figure 2-2 Radial cooling of single pad AFB (a)Schematic of the test bearing (b) Hardware layout for injecting air into bearing, adopted from[2]

Lee and Kim [3] developed 3D thermohydrodynamic (THD) model for air foil bearings under axial cooling as described in Figure 2-3. The bump foil channel was modeled as a plate fin heat exchanger configuration as described in Figure 2-4, where cooling air channels are

consisted of primary and secondary channels. Effective heat transfer resistance from the top foil to the bearing sleeve was measured experimentally and applied to their THD model. Their model predicts the temperature of rotor, top foil, foil structure, bearing sleeve and air film. The temperature of the rotor increases with the decrease in bearing clearance and increases with load and rotor speed. Main heat transfer mechanism in primary channel is convection to the cooling air as shown in Figure 2-4.Cooling effectiveness of secondary channels is lower than that of primary channels because interaction with the heat generated inside the bearing film is through the bump foils which are conduction path to the bearing sleeve. Their study concludes that the clearance change due to foil structure thermal expansion is only a few percentage of the clearance while the rotor's thermal expansion can take up to 20% of the bearing clearance, which suggests the rotor thermal expansion is a primary factor for the thermal runaway of air foil bearings.

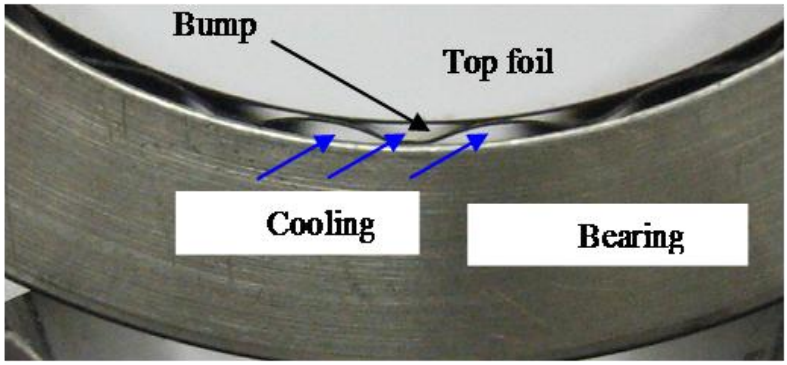

Figure 2-3 Photo showing axial cooling method adopted from [3]

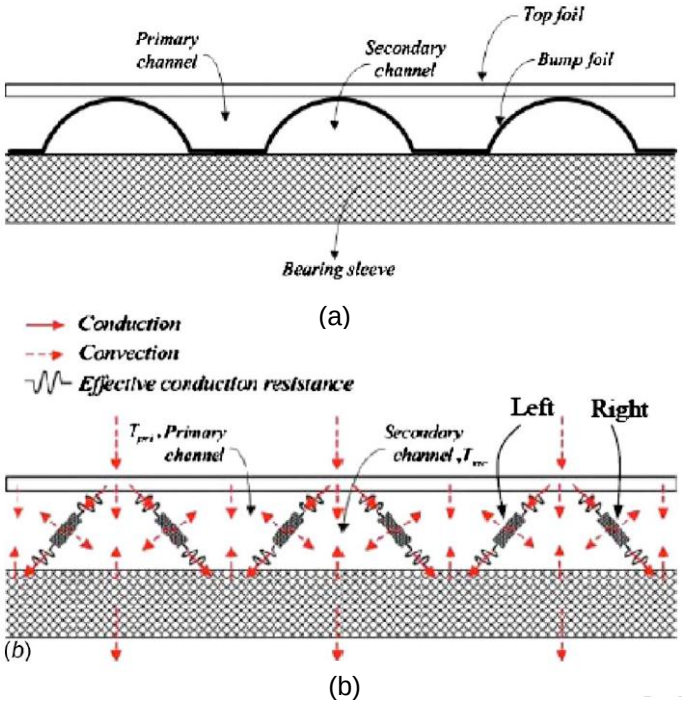

Figure 2-4 Thermal model of foil structure adopted from [3]: (a) foil structure (b) heat transfer mechanism around the foil structure

Kim et al [6] developed a computational model to predict transient thermal behavior of radial three-pad air foil bearings, and also conducted experiments to support their model. They applied transient energy equations to the top foil, bump foil, bearing sleeve, journal shaft, and cooling air itself. The heat generation within the foil bearing and 3-dimensional air film temperature distribution was calculated by solving 3-D energy equation and Reynolds equation at the same time considering all the heat transfer to the top foil, journal shaft, and cooling air flow. It was confirmed from the experiments that the axial cooling is very effective and the amount air flow rate has significant effect on overall transient thermal behavior of the foil bearing. It was observed for the tested foil bearing the axial cooling air pressure difference of 1000pa provided the optimum cooling effect. However, the value can vary significantly depending upon the bearing design and operating conditions.

Radil and Zeszotek [5] conducted different sets of experiments with various speeds and loads. They measured temperature of bearing under these conditions and determined both speed and load are important factor in heat generation in bearing and hence the temperature rise.

Radil et al [7] states that radial clearance plays vital role in performance of air foil bearings. It is concluded from their experiments that the load capacity coefficient (N/mm^3.Krpm) of foil air bearing is directly affected by its radial clearance. The maximum load capacity for given parameters was determined by monitoring torque and shaft speed. As load was gradually increased, rapid increase in torque and decrease in shaft speed were used as an indication of load capacity limit of the bearing. It was noticed that as the clearance increased, the bearing showed better load capacity up to certain value of the radial clearance, but increase of clearance beyond this value resulted in decrease of load capacity coefficient. For low radial clearance, bearing failure occurred due to rise in torque and corresponding decline in shaft speed, i.e., thermal runaway. For bearings with larger radial clearance, it was observed that thermal runaway was not a problem, and the bearings with large clearance would support more load than those with very small clearance. However, too large clearance reduced bearing stiffness and also structural damping could be adversely affected. In overall, increased too large clearance would decrease the bearing's capacity by 20% or less compared to the case with optimum clearance.

Salehi et al [8] performed an analytical and experimental study to obtain thermal characteristics of air foil bearings. They used a Couette flow approximation to the energy equation to calculate theoretical temperature distribution in the foil bearings. They compared their analysis results with the experiments carried out with 100 mm diameter foil bearing at 30,000 rpm max and axial cooling air. It was confirmed via experimental work that Couette flow approximation can be used for certain operation conditions. The paper also points out that

majority of heat transfer during axial cooling occur due to the heat convection between cooling air and the hydrodynamic film.

Kim [9] introduced a new kind of air foil bearing where bump foils were replaced by axially stretched compression springs. One of the advantages of having the compression springs instead of bump foil is controllable stiffness along circumferential direction of bearing (by choosing springs with different diameter, pitch, etc). Also the paper investigates load capacity, structural stiffness and viscous damping of the bearing, which are critical for any kind of bearing design. Both analytical and experimental data were collected to verify spring bumps stiffness with two different cases, i.e., free-free case (0.709MN/m) and clamped-end case (0.858MN/m).Stiffness was estimated by measuring deflection of spring under slow unidirectional load at increment of 2 N up to 22 N. In addition, a new method of bearing cooling was proposed and its effectiveness was investigated by measuring load capacity of bearing with and without cooling effect at 20,000 rpm. Thermocouples were attached at back, centre, and 38.1mm from edge of top foil, and temperature readings from these thermocouples were used as an indication of maximum load capacity of the bearing. 96.3 N was maximum load capacity of the bearing without cooling with temperature rise of about 45^{o}C. However, for cooled bearing, the temperature rise was only 15^{o}C under the same load of 96.3N, proving effectiveness of their cooling channel design.

CHAPTER 3

RESEARCH OBJECTIVE

.One of the main issues of air foil bearings is a thermal management. The objective of this thesis is to investigate radial injection cooling method as a viable alternative option for thermal management of three pad air foil bearings. Background for choosing the radial injection cooling is explained in the following Section 3.1.

3.1 Past Accomplishments

The 3D THD model developed by Lee and Kim [3] was extended by Kim et al [4] to include two cooling air plenums, bearing sleeve, bearing holder, and rotor exposed to the two plenums. As shown Figure 3-4, the cooling air plenums were attached on both side of the foil bearing. The plenum temperatures are unknown because there are thermal interactions with the leakage flows from the bearing and also with the rotor surface exposed to the plenum through convection. The plenum pressures are also unknown because the flow resistance through the bearing is a function of bearing temperature, which is a function of the plenum pressures and temperatures in turn.

In order to solve temperature field of air foil bearings, it is important to know the thermal boundary conditions at the leading edge of top foil described in Figure 3-1. The thermal boundary condition at the leading edge is determined from mass and energy balance equations applied to the region where cooling air is mixed to the leading edge of the top foil. In general, following mixing model was used for the inlet thermal boundary condition;

$$\dot{m}_{mixing} = \dot{m}_{inlet} - \lambda \dot{m}_{exit} \quad \text{with} \quad 0 < < \lambda < 1 \tag{1}$$

$$T_{inlet} = \frac{\lambda \dot{m}_{exit} c_p(T_{exit}) T_{exit} + \dot{m}_{mixing} c_p(T_{mixing}) T_{mixing}}{\dot{m}_{inlet} c_p(T_{inlet})} \tag{2}$$

where λ is defined as a fraction of exit flow that is attached to the rotor surface and recirculated into the next leading edge. From the definition of λ, $\dot{m}_{mixing}$ corresponds to amount of cooling air mixed at the leading edge region, and T_{mixing} corresponds to temperature at the leading edge groove.

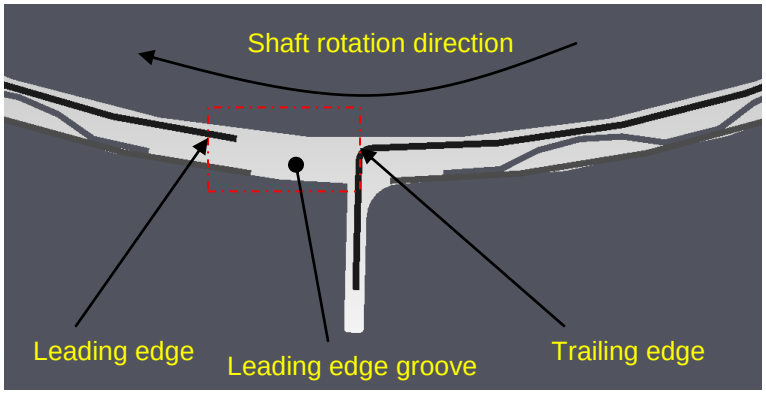

Figure 3-1 Leading edge region

However, λ is generally unknown, and they used computational fluid dynamic (CFD) model on the leading edge region to predict mixing behavior at the leading edge groove. From CFD result, they found λ as a function of injection speed and rotor surface speed as presented in Figure 3-2.

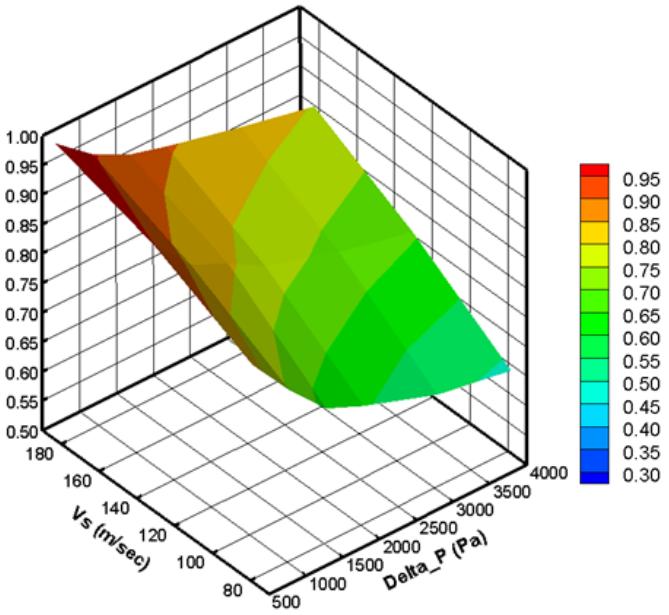

Figure 3-2 λ map for the axial cooling cases from the CFD model, from [4]

Kim et al. [10]compares the simulated THD performance of the three-pad AFBs with single pad circular AFB for different cooling air pressures (up to relatively low cooling air pressure of 300 Pa relative to ambient pressure) assuming $\lambda = 1$. Their results show that, for lightly loaded cases, the three-pad AFBs have lower temperature than single pad bearing. They also compare an ideal case of $T_{inlet} = T_{cooling}$ ($\lambda = 0$ but no axial cooling through bumps) with all the other axial cooling cases (up to 300 Pa) with $\lambda = 1$, and conclude that the ideal case of $T_{inlet} = T_{cooling}$ is the most effective in cooling among all the other axial cooling cases with $\lambda = 1$. However, it is noteworthy the comparison was with relatively very small cooling air pressure of only 300 Pa.

As mentioned above λ=0 is an ideal case which can be achieved if thermal boundary layer can be completely broken by cooling air injection to the leading edge of top foil directly. However, the ideal case of λ=0 is not possible, and the most practical way to achieve the case

of λ=0 is to inject very high speed cooling air on to the rotor surface at the leading edge groove area. As noted earlier, the work by Radil and Batcho [2] used a single point injection at low speeds and also the tested air foil bearing was with single top foil.

3.2 Present Goal

The most common method of foil bearing cooling has been axial cooling due to easiness in adopting the method as no special hardware modification is necessary to the bearing. Bump channels serve as a heat exchanger, and reasonable effectiveness is achieved via supply of cooling air along the axial direction as shown in Figure 2-3.However, mixing of supplied cooling air to the leading edge of the top foil is minimal because λ~1 as presented in [4].

From previous studies conducted in [3, 4, 10, and 11], it is concluded that thermal boundary condition at the leading edge of top foil could determine bearing overall temperature. Kim et al [4] conducted CFD analysis to evaluate numerical value of recirculation ratio, and deduced that lower value of λ could facilitate in minimizing bearing mean temperature. It is noteworthy that ideal value for λ is zero, which is not possible in practice. Hence, the idea of reducing λ value was developed by directly injecting air jet in the shaft in the leading edge groove region. So that the mixing of air could be increased and the temperature of air at the leading edge could be reduced as much as possible. Also Reference [3] evaluated that the thermal and centrifugal growth of the rotor contributes to 20% of clearance change, suggesting the thermal expansion of the rotor could potentially be the main cause of thermal runaway of foil bearings. In that regard, radial injection of cooling air on to the shaft may have direct cooling effect of the shaft.

This thesis compares the commonly-used axial cooling method with multiple radial cooling air injection onto the rotor surface at the leading edge region of three pad air foil bearing. Unlike the single pad foil bearing, the three pad foil bearings can implement radial air

injection cooling at multiple locations (along circumferential direction). The motivation of the study on the radial injection comes from the preliminary THD study on three-pad AFB [10] as mentioned in the previous section, where they suggest that maintaining the leading edge temperature as that of the cooling air is more effective than passing cooling air axially under small pressure gradient up to 300Pa.

Hence, the idea of the air impingement directly to the rotating shaft could be a feasible option, and its cooling effectiveness is evaluated in this thesis.

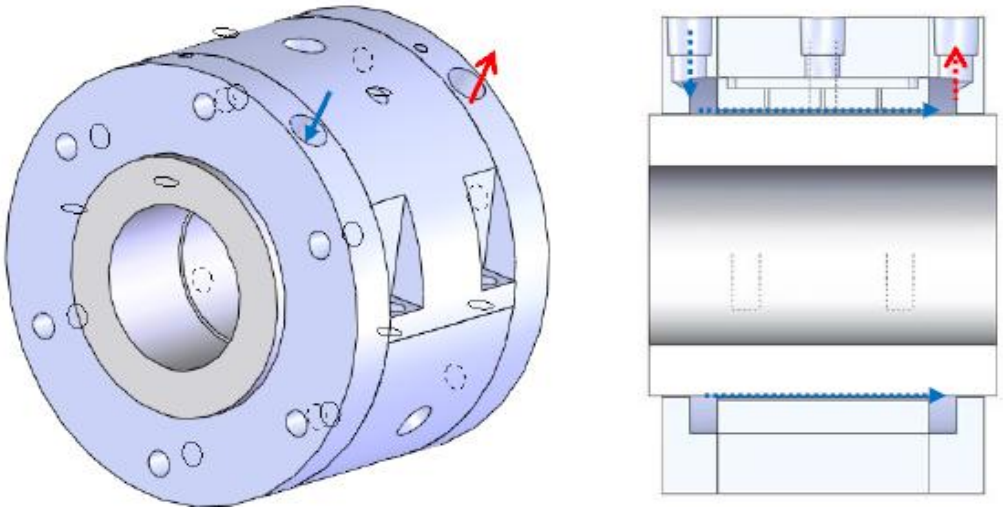

Figure 3-3 Air flow direction in axial cooling with plenum configuration

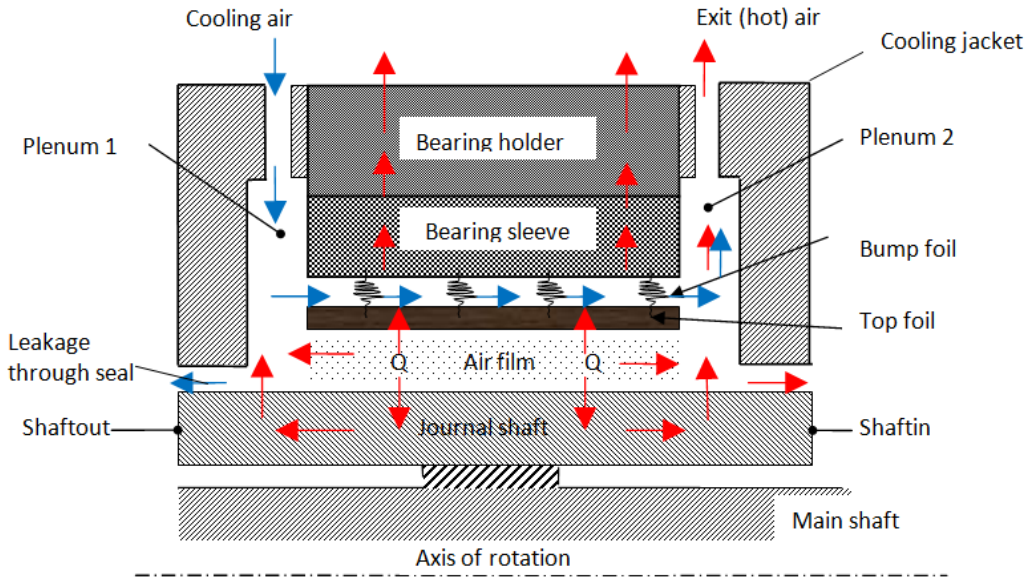

Figure 3-4 Heat transfer mechanism in axial cool method, blue arrow represents cooling air and red arrows represent hot air

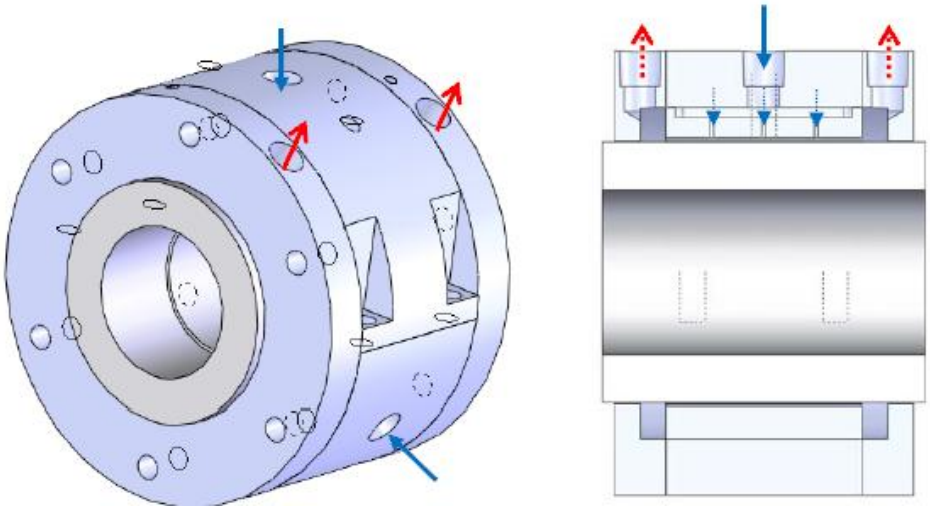

Figure 3-5 Air flow direction in radial cooling

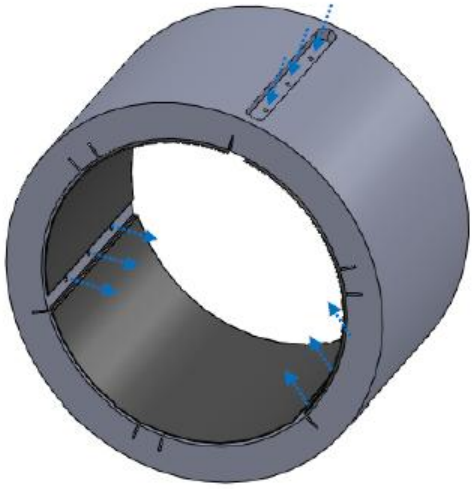

Figure 3-6 AFB with radial injection holes at the leading edge region

CHAPTER 4

EXPERIMENTAL SETUP

This chapter explains the hardware modification to test radial injection cooling and instrumentation to collect the experimental data. Figure 4-1 shows CAD model of actual test rig configuration.

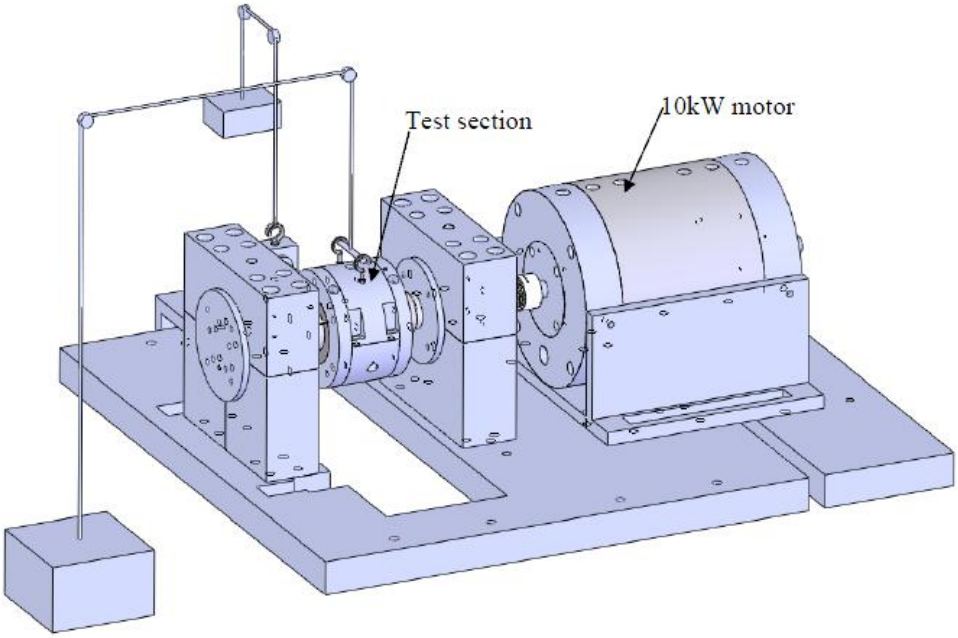

Figure 4-1 Test Rig configuration

4.1 Hardware Set Up

Changes were made to the bearing sleeve in order to accommodate the radial cooling method. Further details on these adjustments are mentioned in section below.

4.1.1 Pressure Transducer

Pressure Transducers (PX409-2.5G5V) from Omega, Inc. were used to measure the plenum air pressures at both inlet air plenum 1 and exit air plenum 2. Figure 4-2 shows the 10VDC power source for the transducer. The voltage signal from the transducer was processed through the NI 9205 Input module. This module was then attached to the CDAQ-9174 chassis which was connected to the computer via USB. Custom-built LabVIEW VI was used to process the voltage signal to pressure. Following equations(3) and Figure 4-3 were used to calibrate the transducer voltage and actual pressure.

$$\text{Pressure} = \underbrace{(output)}_{voltage} \times (0.0345)\, psi / volt + offset \tag{3}$$

The values used in equation(3) were derived from the calibration certificates provided by the manufacturer.

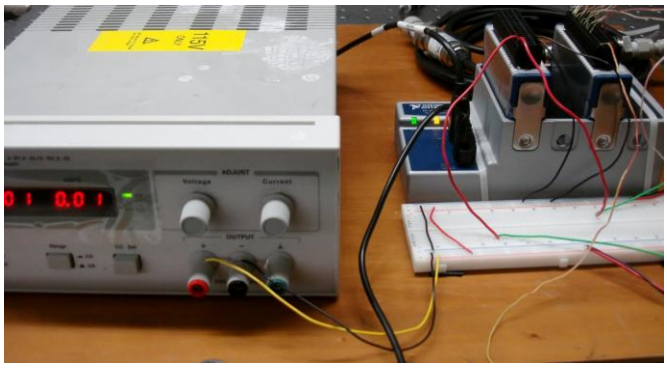

Figure 4-2 DC power source used for the pressure transducers

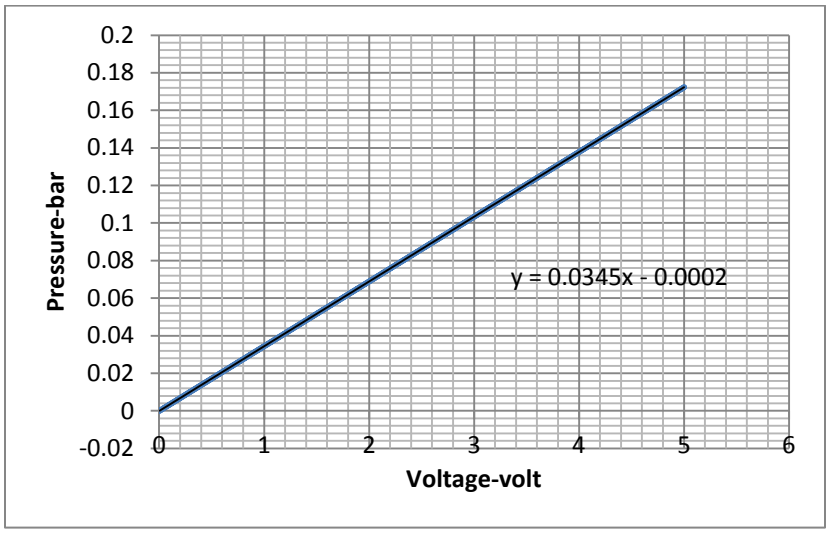

Figure 4-3 Pressure -Voltage Calibration curve

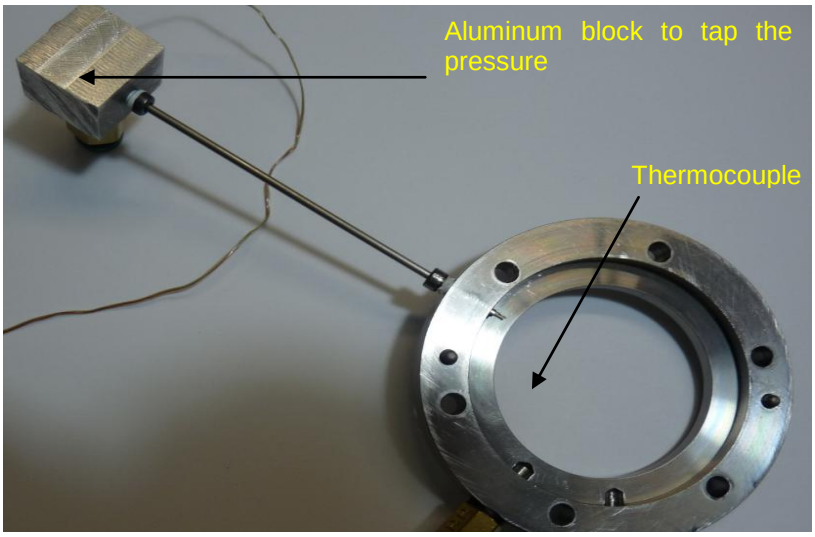

Figure 4-4 Cooling jacket with thermocouple and aluminum block to tap pressure inside the plenum

4.1.2 Temperature Measurement

Thermocouples were used to measure the temperature of bearing sleeve, bearing holder, air inside the both plenums, and two ball bearing housings. The temperature data were collected using National Instruments device NI 9213.This thermocouple module was then

attached to the NI chassis cDAQ-9174 which contains the system's data, timing and triggering buses. The chassis was connected to the computer via USB port and the LabVIEW VI was built to store and display the real time temperature data. Figure 4-5 shows the LabVIEW VI displaying temperature and Pressure in degree Celsius and Pascal unit in real time.

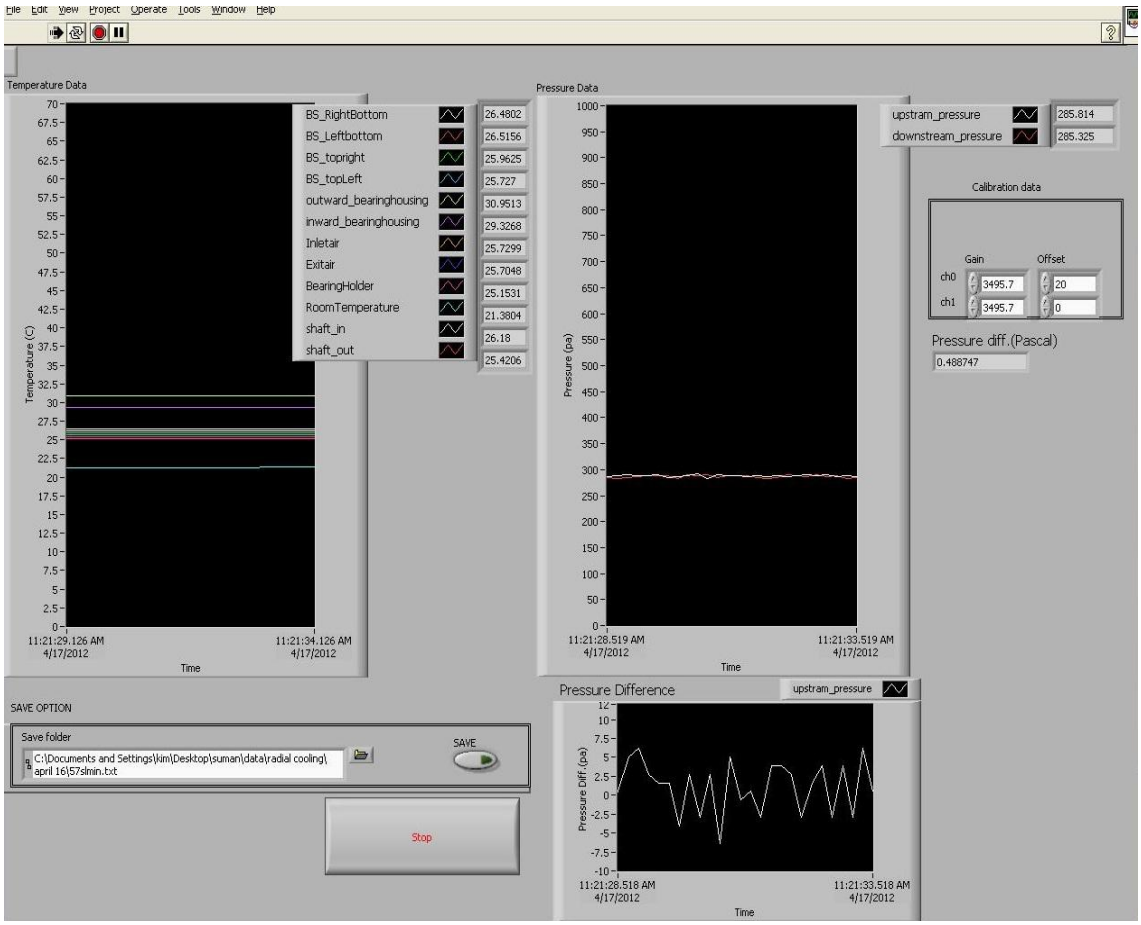

Figure 4-5 LabVIEW window used to measure the temperature and pressure data of the bearing

4.1.3 Torque Monitoring

In order to prevent sudden failure and damage to the test rig, preventive method was followed. A (torque) rod of the length 120mm was attached to the bearing holder as shown Figure 4-7 where the bearing friction force transmitted to PCB 201B01 load cell via the torque rod. Figure 4-6 shows the screen shoot of LabVIEW used for torque monitoring using the load

cell. Output voltage signal from load cell was converted to the torque signal using Table 4-1 and equation(4).

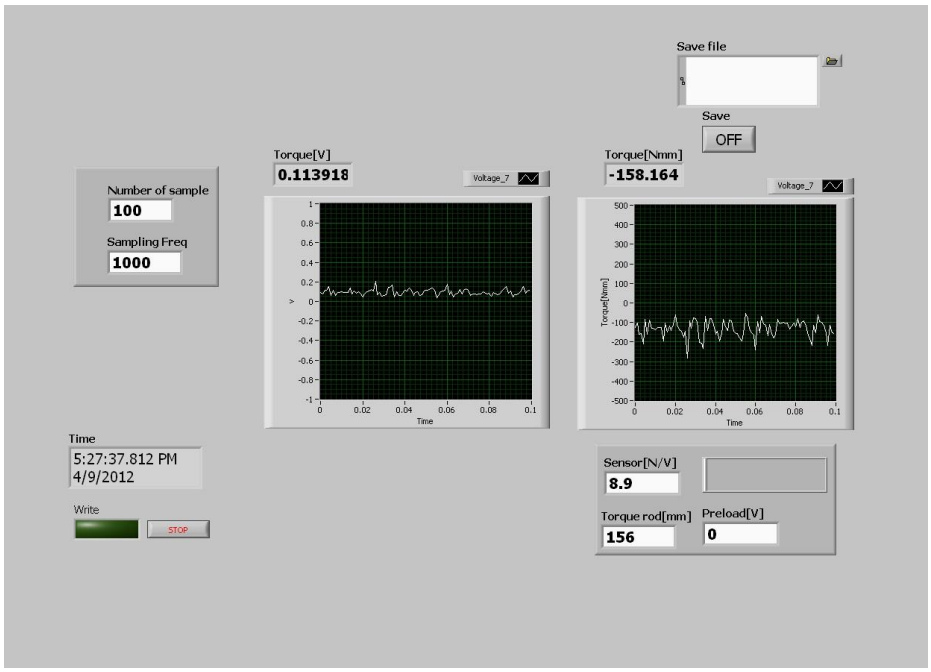

Figure 4-6 LabVIEW window used to monitor the torque due to friction force in AFB

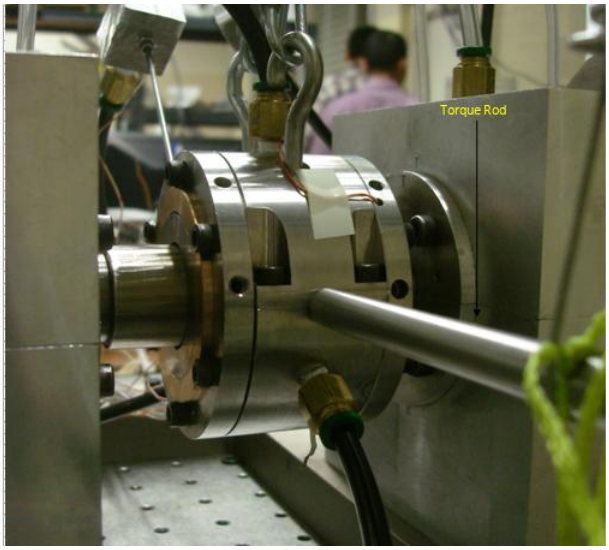

Figure 4-7 Torque rod attached to bearings holder for friction force monitor in the bearings

Table 4-1 Load Cell Calibration Data

Model	Measurement Range	Sensitivity	Preload	Temperature Range
201B01	10LB	500mV/lb	60lb	-54 to +121^{o}C

$$Torque = \underbrace{(output)}_{voltage} \times \frac{1}{(sensitivity)} \times \underbrace{156mm}_{(TotalLength)} \quad (4)$$

4.2 Test Rig Configuration

The test rig is consisted of in-house built 10kW induction motor with rated speed of 70,000rpm, two ball bearing housings with GMN high precision ball bearings, torque rod with preloaded PCB load cell, and loading mechanism for the AFB. A high precision flexible coupling balanced to maximum 100,000rpm is used to connect the motor shaft and the main test shaft as shown in the Figure 4-8 (b). The test journal shaft is press fitted onto the main shaft through a ring adapter (SS 316) at the center as shown in Figure 3-4.Hence there is very narrow contact area between the main shaft and the journal shaft, which allows very little heat transfer to/from the main shaft. This setup was necessary to isolate the journal shaft as much as possible from external heat source (ball bearing friction power loss) so that identification of thermal boundary conditions on the shaft could be easier. The whole test rig sits on a vibration isolation table. Figure 4-8 (a) shows the test rig configuration.

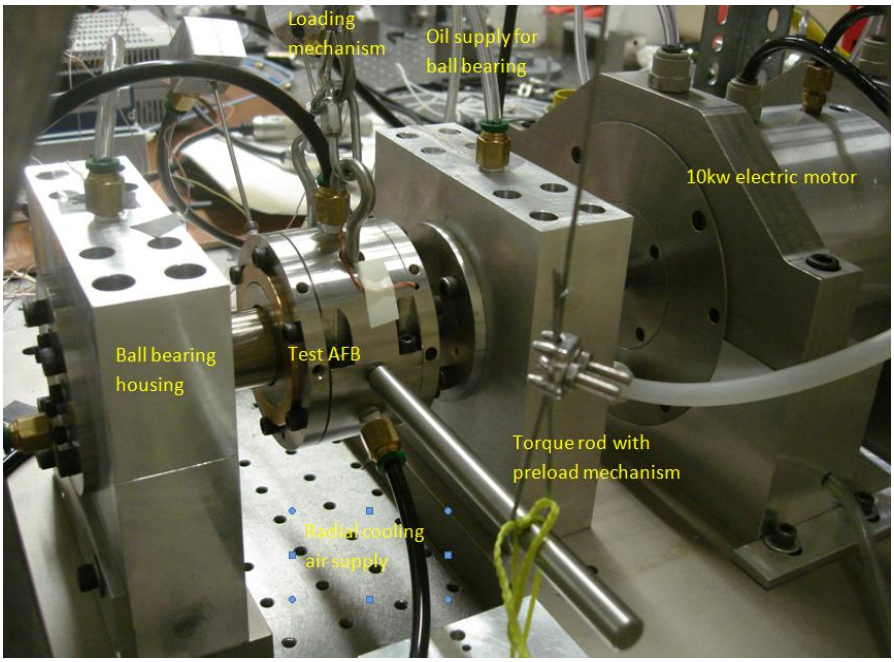

(a)

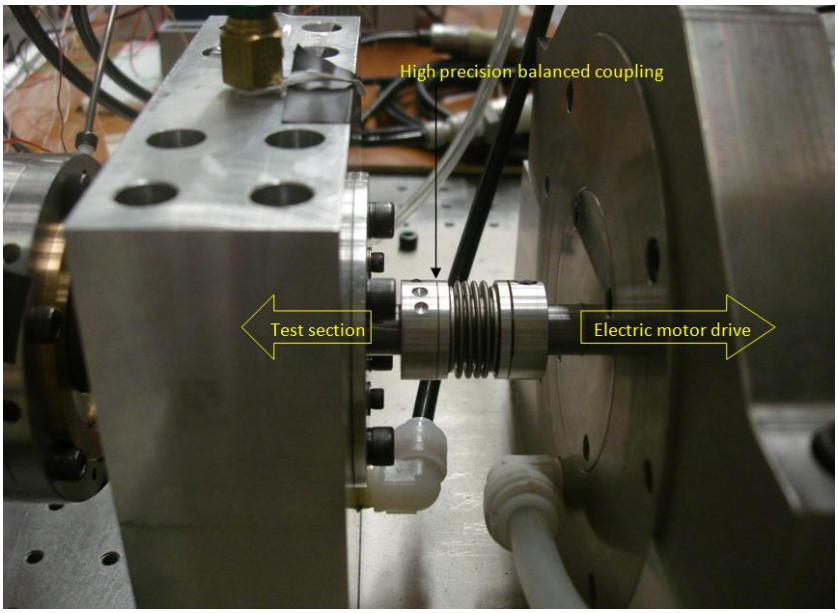

(b)

Figure 4-8 (a) Test rig configuration (b) Coupling between motor and test section

4.2.1 10 KW Electric Motor

In the previous work by [12], a small 2KW motor was used for the similar experiments. However, it was observed that the torque required for the rig to run at higher speed wasn't enough. Hence a new 10KW motor was designed with higher torque. All the motor parts were designed by Dr. Kim and machined at UT Arlington machine shop in Woolf Hall except the motor rotor element and stator coil, which were purchased.

The speed of the motor was regulated by a frequency converter, FC 80 series, from SIEB & MEYER, Inc. Alemite 3920 oil mist lubricator was used to lubricate the four ball bearings in the electric motor and test section.

4.2.2 Test Bearing

The test foil journal bearing is the hydrodynamically pre-loaded three-pad foil bearing with higher stability then typical single pad AFBs. Figure 4-10 (a) shows the three-pad AFB with preload and Figure 4-10(b) shows the photo the actual test bearing with the thermocouples and bearing holder attached. It is consisted of three top foils with each top foil supported by independent bump foils underneath and these bump foils are spot welded on to bottom foils .The use of bottom foil may seem redundant but the original idea of having bottom foil was easiness in removal and placement of bump foils to the bearing sleeve. It was experienced through the course of this research that proper assembly of bottom and top foils on to the bearing sleeve s very important for the bearing to function properly. Figure 4-9 shows how top foil, bump foil and bottom foil are arranged. To reduce the torque during start/stop, the top foils are coated with Teflon as shown in Figure 4-12 (c).

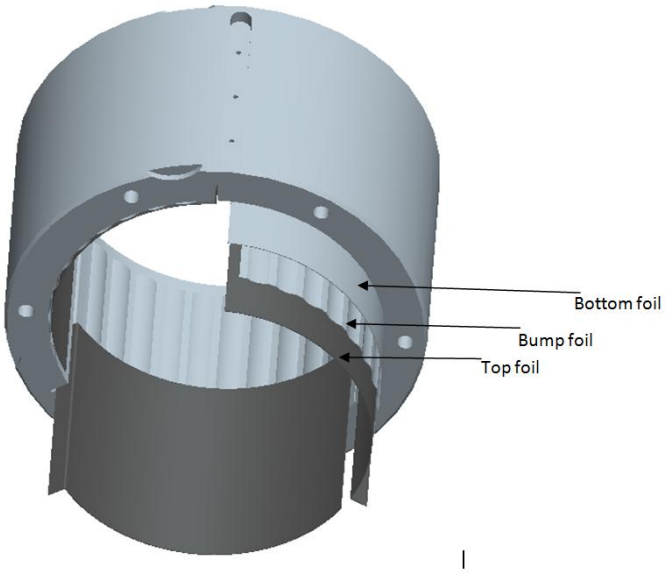

Figure 4-9 AFB with arrangements of top foil, bump foil and bottom foil

Table 4-2 Specification of the AFB used (unit: mm)

Rotor radius	24.5
Bearing length	37.5
Bearing radius	24.585
Top foil thickness	0.127
Bump foil thickness	0.127
Bump height	0.49
Nominal clearance(C)	0.120
Set Bore clearance(C_S)	0.085

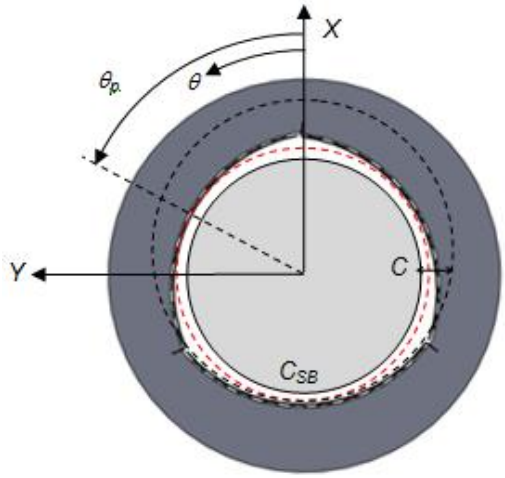

(a)

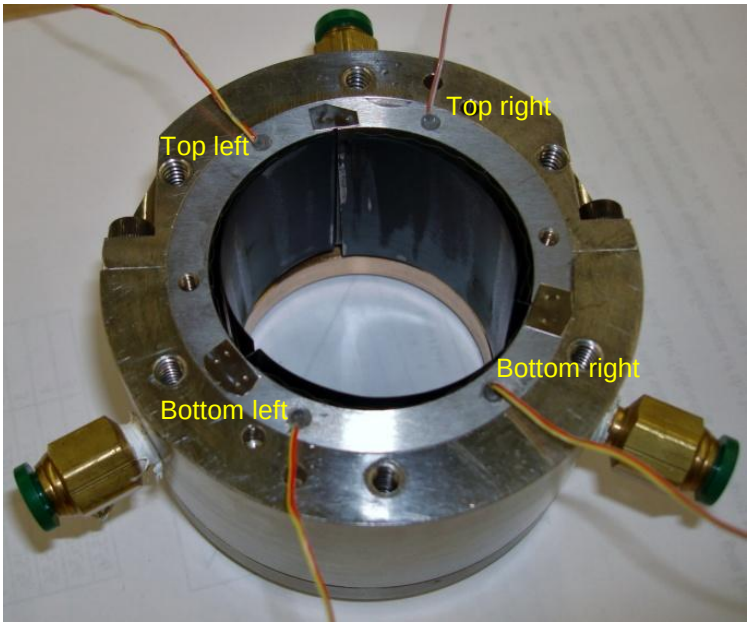

Figure 4-10 (a)Three-Pad AFB with preload (b) photo of the AFB with bearing holder and thermocouples attached

4.3 Fabrication of The Bearing Components And Foils

The bearing components comprise bearing sleeve, top foil, bump foil and bottom foil. Bearing sleeve was manufactured with EDM process outside the lab. Bearing sleeve has three

locations for the radial injection holes as shown in Figure 3-6. The diameter of the injection hole is 0.75 mm and they are placed between the leading and trailing edge of the top foils.

Foils were made of annealed 125 microns thick Inconel X750, and they were formed into required shape using a custom designed jigs and age-hardening process following the heat treatment curve shown in Figure 4-11

Top is actual bearing surface. Since the rotor reside on top foil, it is important to maintain curvature and shape of these foils without any indentation. Also it was noted during the course of research that lip of top foil (see Figure 4-12C) shouldn't be constrained in the slots rather be free to move in the slot that is they should be free. For the purpose of this experiment, all of the top foils were Teflon coated. Following steps were followed to fabricate the top foils.

A blank sheet metal of 0.127mm thickness was cut into 52.5 mm x 37.5 mm. This sheet metal was then formed to get the required curvature and shape by using custom made jig and hydraulic press. Figure 4-12 shows the blank sheet metal and the top foils. As the annealed Inconel is ductile, heat treatment of the top foil was done following the heat treatment curve shown in Figure 4-11.

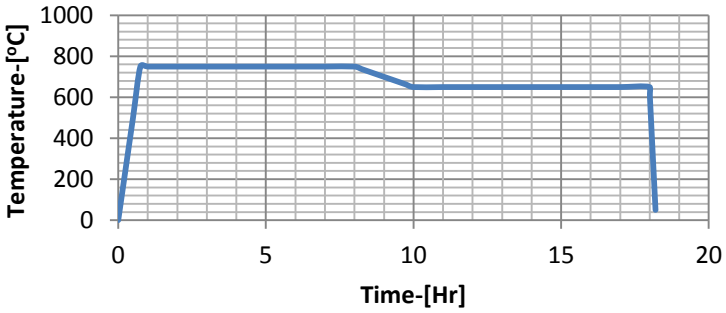

Figure 4-11 Heat treatment curve of the Inconel X750

Similar procedure is followed for the bottom foils except the lip area of bottom foils were removed and were directly welded onto the bearing sleeve.

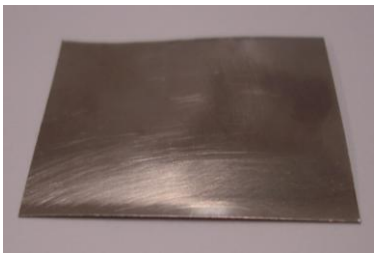

(a)

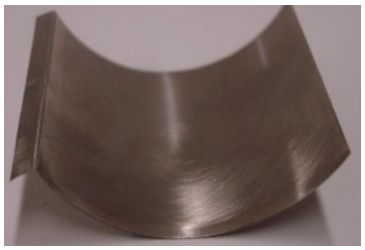

(b)

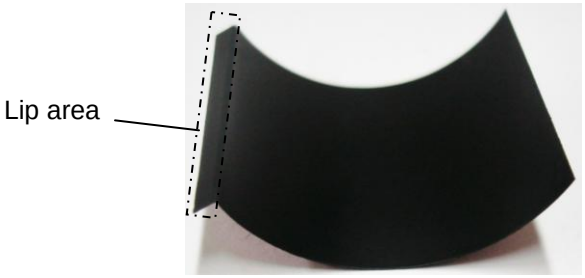

(c)

Figure 4-12 Fabrication of Top Foil (a) Blank sheet metal (b) Uncoated Top Foil (c) Teflon coated Top Foil

Bump foils are the corrugated shape sheet metal that lies under the top foil. These foils provide the necessary stiffness and damping to the bearing and are responsible for the bearings stability and performance.

Similar to top foil, a blank sheet metal is cut into 50 mm x 35.5 mm and required corrugated shape as shown in Figure 4-13 (a). The shape of the bump foil is formed by giving it a curvature as shown in Figure 4-13(b) using a 1.5” diameter mandrel. A careful handling of the bump foil is necessary at this stage because bump foils can easily lose their shape accuracy, especially the height leading and trailing bumps.

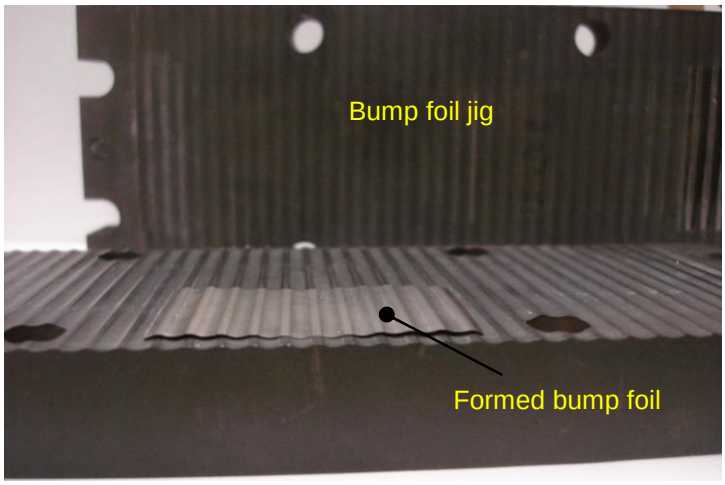

(a)

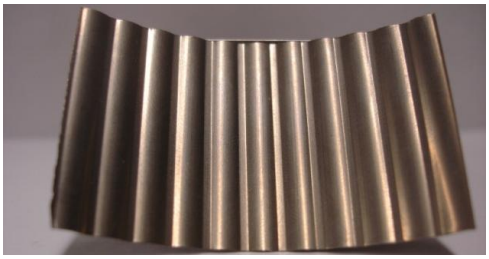

(b)

Figure 4-13 (a) Bump Foil jig with formed bump foil (b) Bump Foil with curvature

CHAPTER 5

RESULTS AND DISCUSSION

5.1 Purpose of The Experiment

Sets of experiment were performed with 30krpm and 10lb load. Focus of the thesis was to operate the experiment under various air injection speeds for radial cooling and corresponding flow rate for axial cooling method, and evaluate the both cooling methods.

5.2 Determination of Air Flow Rate For Radial Cooling Method And Corresponding Axial Cooling Flow Rate

Air flow rate plays an important role in determining the cooling effectiveness of the bearing. Therefore it is necessary to maintain the same amount of air flow rate for the both cooling methods. The amount of flow rate was calculated in reference to the rotor surface speed (V). Equation (5) and (6) were used to calculate the required mass flow rate for radial cooling.

$$V = r \times \underbrace{2 \times \pi \times Ns}_{(\omega)} \tag{5}$$

Where N_s is the rotor speed in rpm, r is radius of the rotor, and V is surface velocity of the rotor.

$$\dot{m} = \rho \times A \times V \tag{6}$$

Where $\dot{m}$ is mass flow rate, ρ is density of air, and A is area of the injection holes. To compare various cases, the mass flow rates were calculated using 150%, 200%, 250% and 310% of rotor surface speed. And equivalent mass flow rates were used for axial cooling method.

Table 5-1 shows the calculated values of flow rate for the radial injection case.

Table 5-1 Flow rate calculation of radial injection

No. of holes	9	
Radius(R)	0.000375	m
Density(ρ)	1.176829	Kg/m^3
Area(A)	4.42E-07	m^2
V	76.96902	m/s
$\dot{m}$	0.00036	Kg/s
$\dot{Q}$	18.23968	SLPM

The supplied air for axial flow is leaked through seal clearance area as shown in Figure 3-4 which makes it hard to know the exact amount of mass flow rate across the bearing. Figure 3-3 and Figure 3-5 show the flow directions of cooling air for axial and radial cooling respectively. An experiment was carried out under the static condition mimicking that of axial cooling method to measure the pressure drop across two bearing for different mass flow rates with seal clearance blocked.

Table 5-2 shows the flow rate vs. pressure difference, and Figure 5-1 shows the data in graph. Equation (6) is the relation between pressure difference and flow rate interpolated from the graph. This equation was used to calculate the pressure required across the bearing to have certain flow rate for axial cooling.

$$\underset{Pressure}{dP} = 0.0509\times(\dot{m})^2 + 14.84\times(\dot{m}) \qquad (6)$$

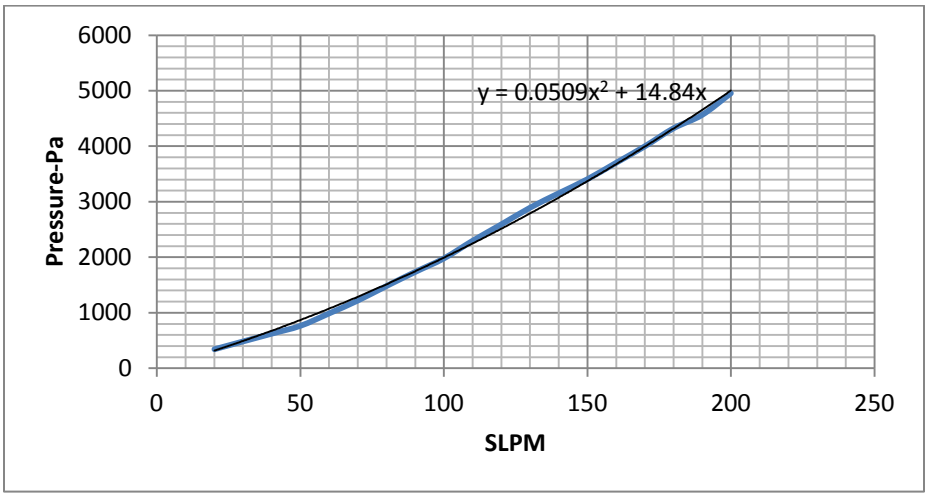

Figure 5-1 Pressure drop vs. Flow rate in static Axial Cooling

Table 5-2 Measuring Pressure drop for different Flow rates

SLPM	Pressure difference-(pa)
20	339.15
30	480.49
40	620.62
50	762.42
60	986.03
70	1218.41
80	1480.06
90	1733.92
100	1978.23
110	2295.91
120	2591.08
130	2891.94
140	3152.44
150	3406.15
160	3702.27
170	3998.80
180	4323.99
190	4566.41
200	4955.90

5.3 Temperature Variation Due To Different Mass Flow Rate

Series of experiments were performed for the both radial and axial cooling methods with different mass flow rates. Following discussion includes explanation on data measured with corresponding figures.

5.3.1 Bearing Sleeve Temperature

Figure 5-2 shows the effect of mass flow rate in bottom bearing sleeve temperature with radial and axial cooling respectively. It can be seen that both cooling methods are affected by flow rate and shows improvement in cooling effectiveness as flow rate is increased. Similar trend is followed by top bearing sleeve temperature as shown in Figure 5-3.

The increased cooling effectiveness with higher pressure difference across the bearing for axial cooling is combined effects of increased cooling air flow rate through the bump channels and also decreased (cooling) air temperature in plenum 1.Similarly higher flow rate value for radial injection increased the cooling effectiveness. Higher flow rate values correspond to increased injection speed of the impinging air, easily breaking the thermal boundary layer of the rotor.

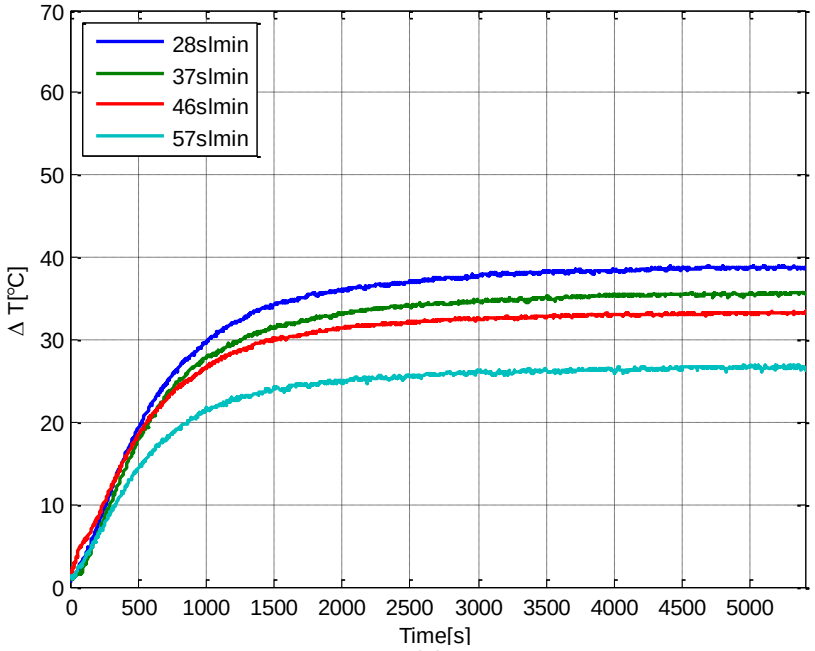

(a)

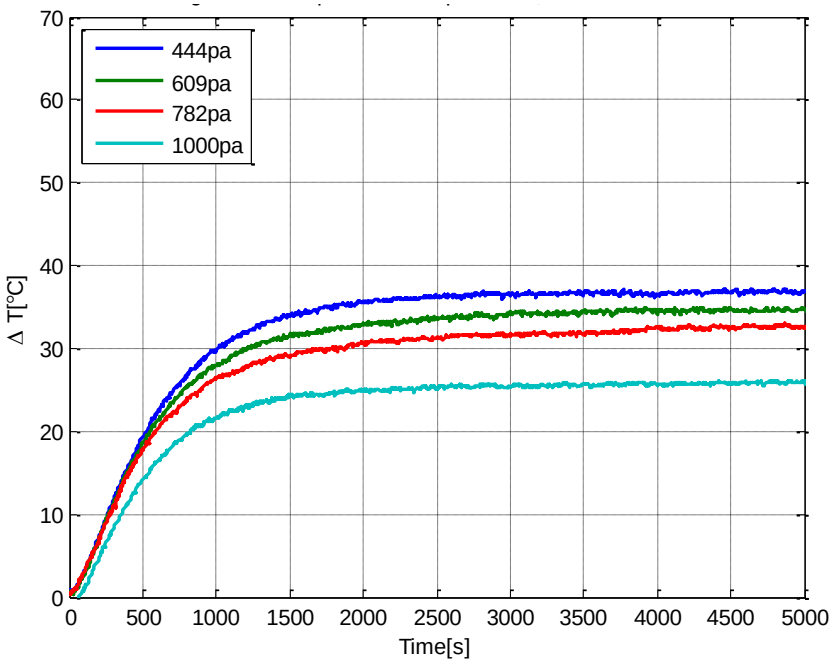

(b)

Figure 5-2 Transient behavior of Bottom bearing sleeve temperature distribution with different flow rates(a) Radial cooling (b) Axial Cooling

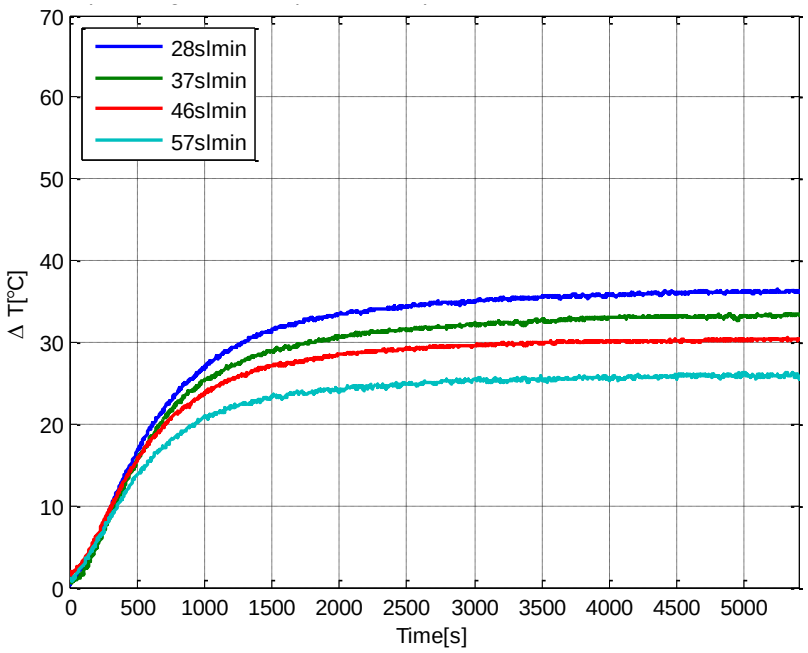

(a)

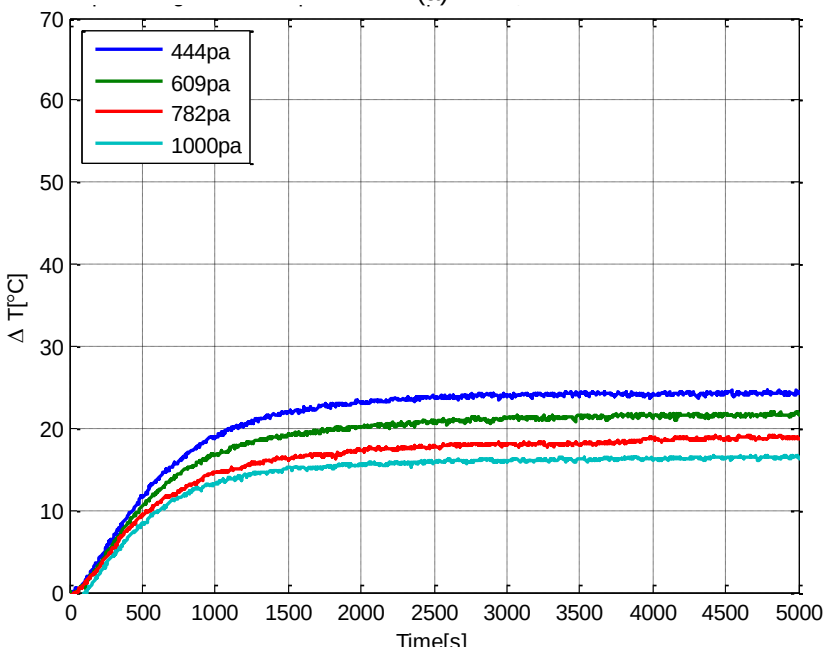

(b)

Figure 5-3 Transient behavior of Top bearing sleeve temperature distribution with different flow rates (a) Radial cooling (b) Axial Cooling

5.3.2 Plenum Air Temperature

Cooling jackets were attached on both sides of the bearing sleeve. For axial cooling, air is supplied to plenum 1 which distributes the cooling air to the bump channels. Exit air from the bump channels is collected at plenum 2 from where it escapes to the environment.

Aluminum blocks as shown in the Figure 4-4 were used to measure the temperature and pressure in the both the plenums. As presented in

Figure 5-4 and Figure 5-5 the steady state temperature for inlet and exit air varied with the air flow rate. Higher flow rate increased the effectiveness of both radial and axial cooling method.

5.3.3 Bearing Holder Temperature

Similar to above mentioned trend, bearing holder temperature was directly proportional to the flow rate. Since the holder is exposed to the environment the mean temperature of the holder was lower than other bearing components. Figure 5-6 (a) and (b) displays the bearings holder temperature at different flow rates and cooling methods, radial and axial respectively.

5.3.4 Ball Bearing Housing temperature

Even though the temperature measurement of ball bearing housing was not used to reach any conclusion, the temperature monitoring of the housing was necessary to confirm the proper functioning of the rig. The measurements done as shown in the Figure 5-7 (a) and (b) validate the statement that bearing parameter and running conditions were identical regardless of the flow rate applied or the cooling method implemented

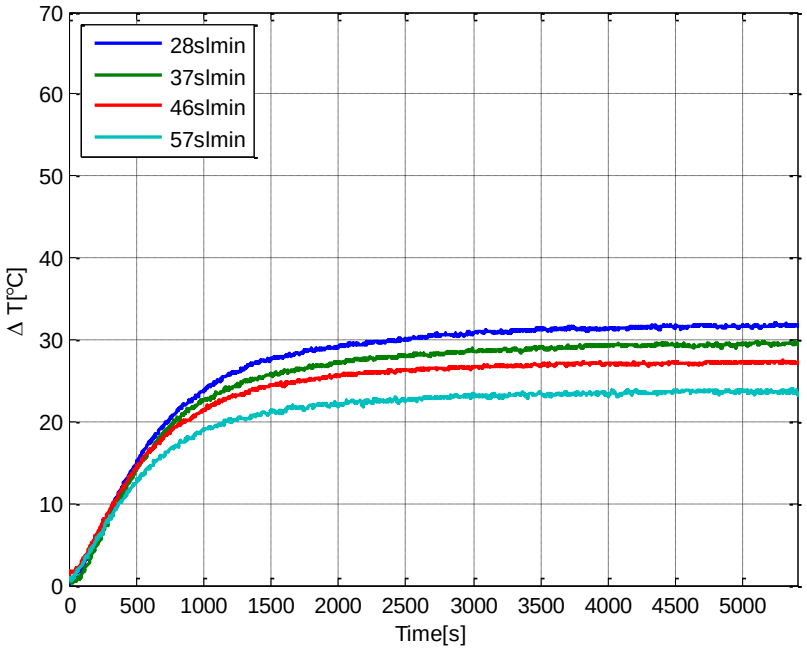

(a)

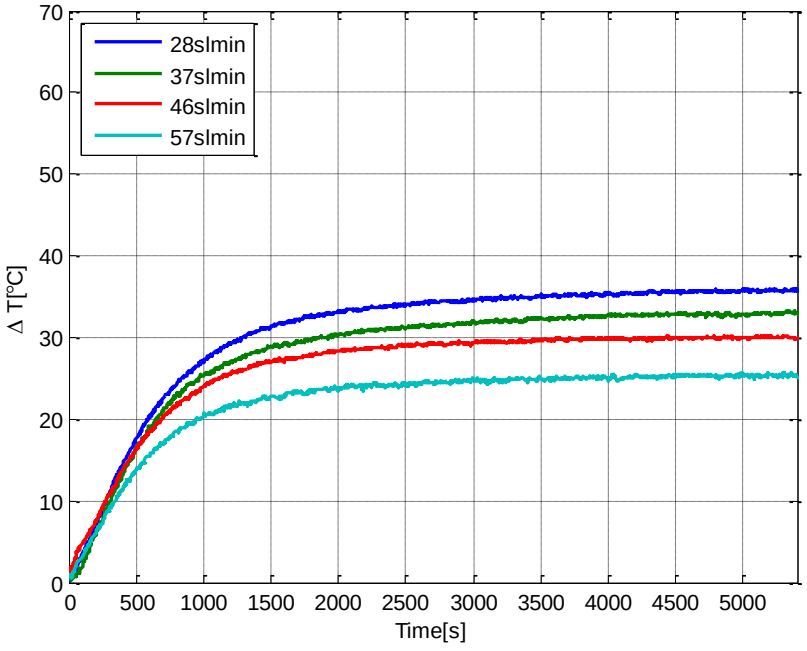

(b)

Figure 5-4 Transient behavior of plenum temperature at different mass flow rates and radial cooling method (a) Plenum 1 (b) Plenum 2

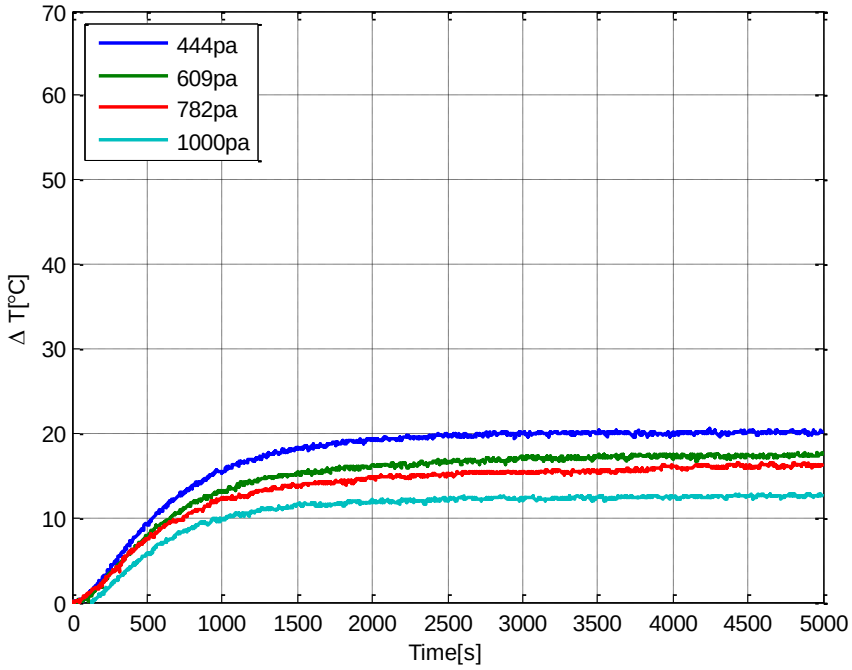

(a)

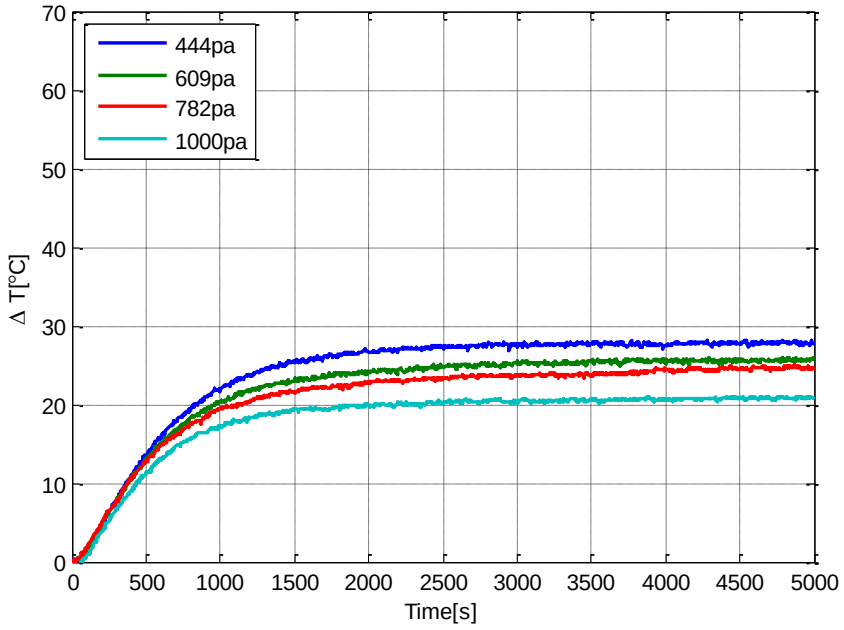

(b)

Figure 5-5 Transient behavior of plenum temperature with different mass flow rates and axial cooling method (a) Inlet air-Plenum 1 (b)Exit air- plenum 2

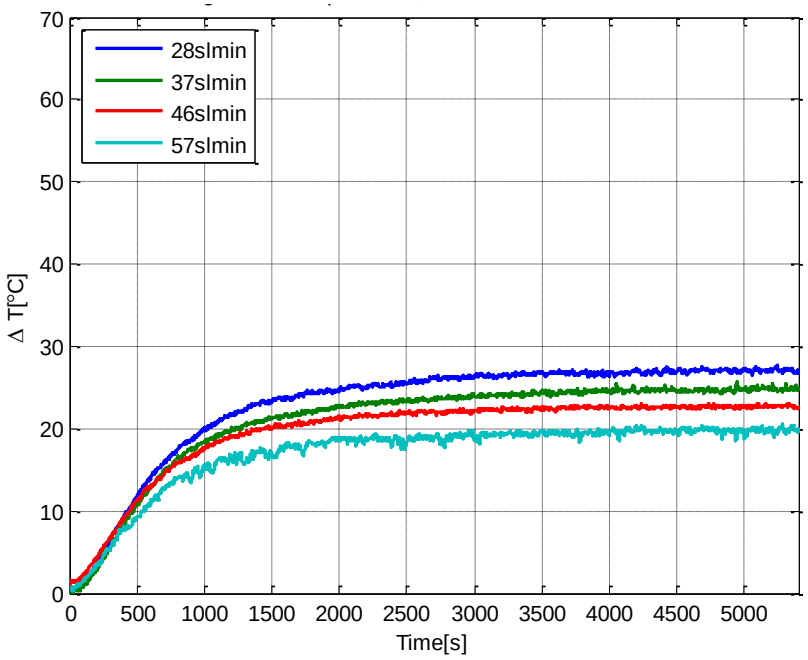

(a)

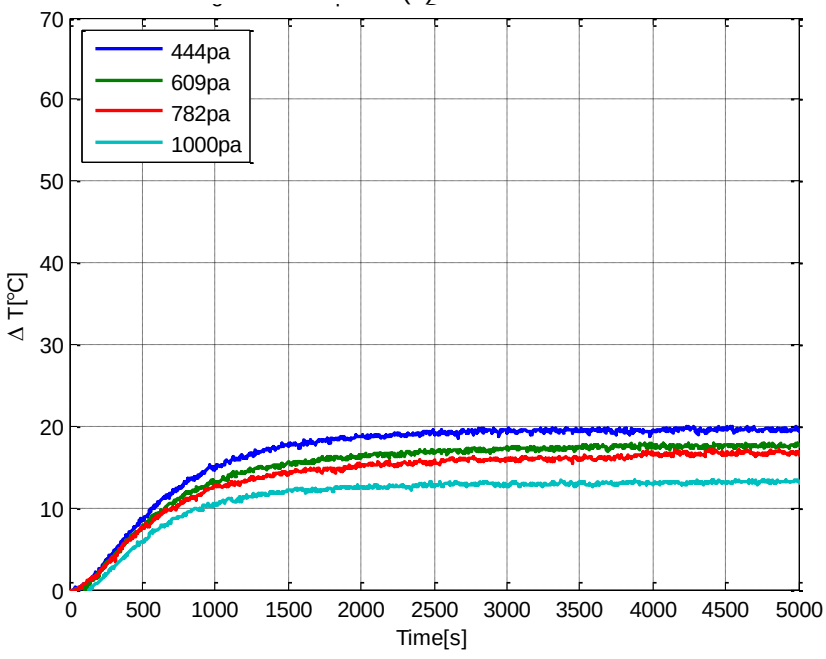

(b)

Figure 5-6 Transient behavior of Bearing holder temperature with difference mass flow rates(a)radial cooling method (b)axial cooling method

.

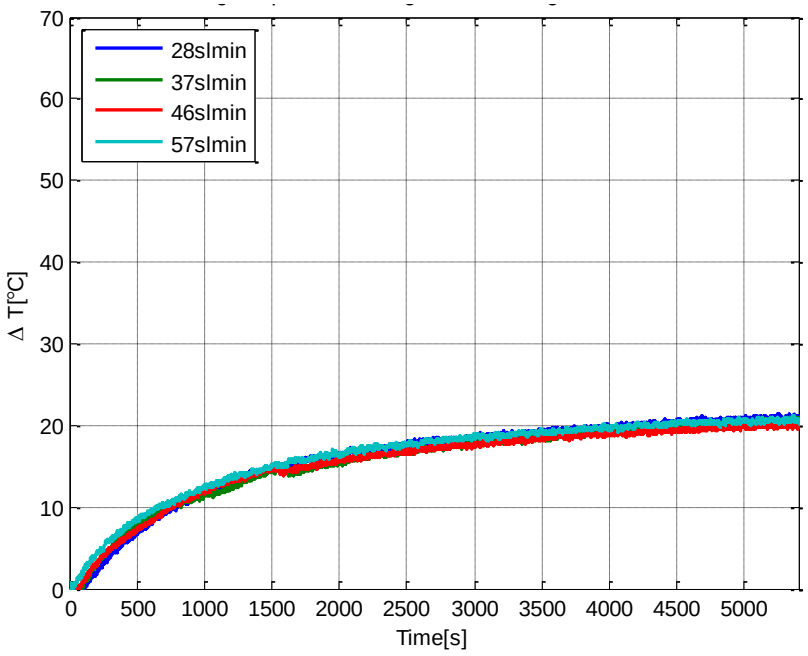

(a)

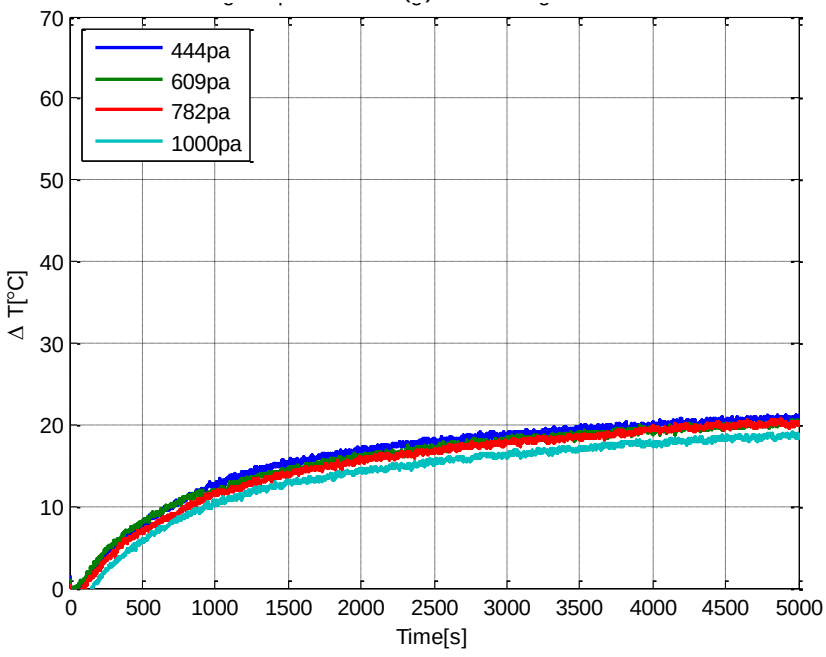

(b)

Figure 5-7 Transient behavior of Ball bearing housing temperature with (a) radial cooling (b) axial cooling

5.4 Temperature Variation Due To Different Cooling Methods

Four sets of tests were performed, for each set two experiments were conducted with radial and axial cooling techniques using similar flow rate value (four different flow rate values tested).Temperature data were used to conduct the following analysis and comparison.

5.4.1 Bearing Sleeve Temperature Comparison

Bearing sleeve temperature were measured at four different locations as shown in the Figure 4-10(b).It can be observed from Figure 5-8 that the mean bearing sleeve temperature for radial injection method is higher. However, the thermal gradient for radial cooling is lower compared to axial cooling method. This trend is repeated for all four flow rate values used for this experiment as shown below in Figure 5-8 through Figure 5-11.

The lower mean temperature of bearing sleeve for axial cooling is due to heat transfer between the cooling air flowing through the bump channels and heat generated. In radial cooling, air is injected to the leading edge groove region; cooling effect is limited to the lead edge region of top foil. It is speculated that as air starts to circulate further away from the leading edge region, temperature rapidly increases demeaning the significance of air injected in the region. Hence, the bearing sleeve is subjected to higher mean temperature. However, the radial injection method showed lower thermal gradient of the bearing sleeve in circumferential direction. The sleeve consists of three different injection points 120^{o} apart with three .75mm holes at each point.

The overall temperature of the bearing sleeve may be slightly higher but radial cooling method maintains difference between the top and bottom bearing sleeve temperature to be within $5^{o}C$, unlike the axial cooling which has the average temperature difference of $10^{o}C$ or more.

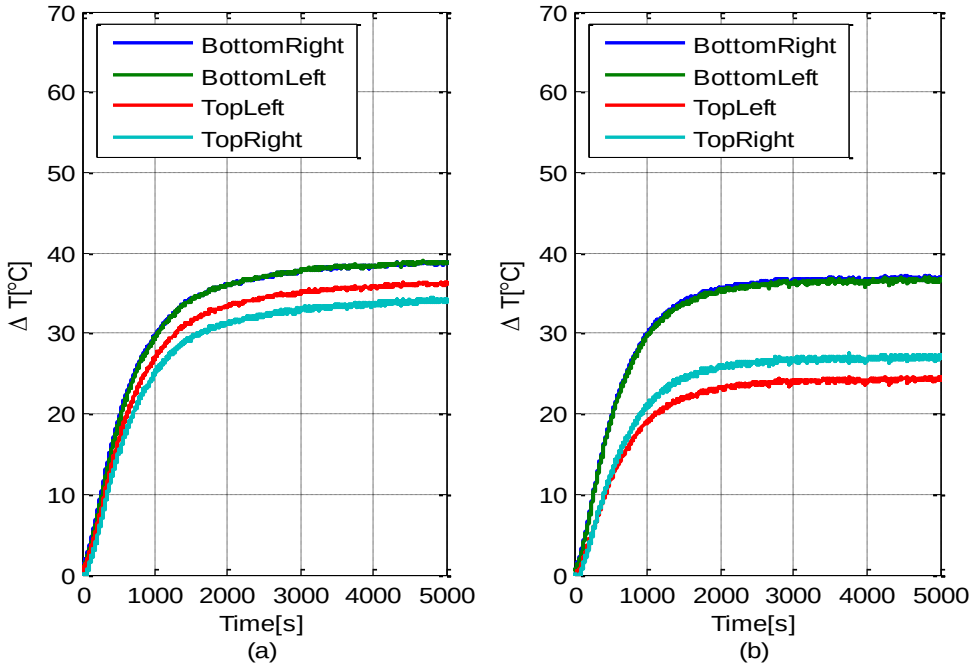

Figure 5-8 Transient behavior of Bearing sleeve temperature distribution at 28SLPM (=444pa pressure difference along axial direction) (a) Radial cooling (b) Axial cooling

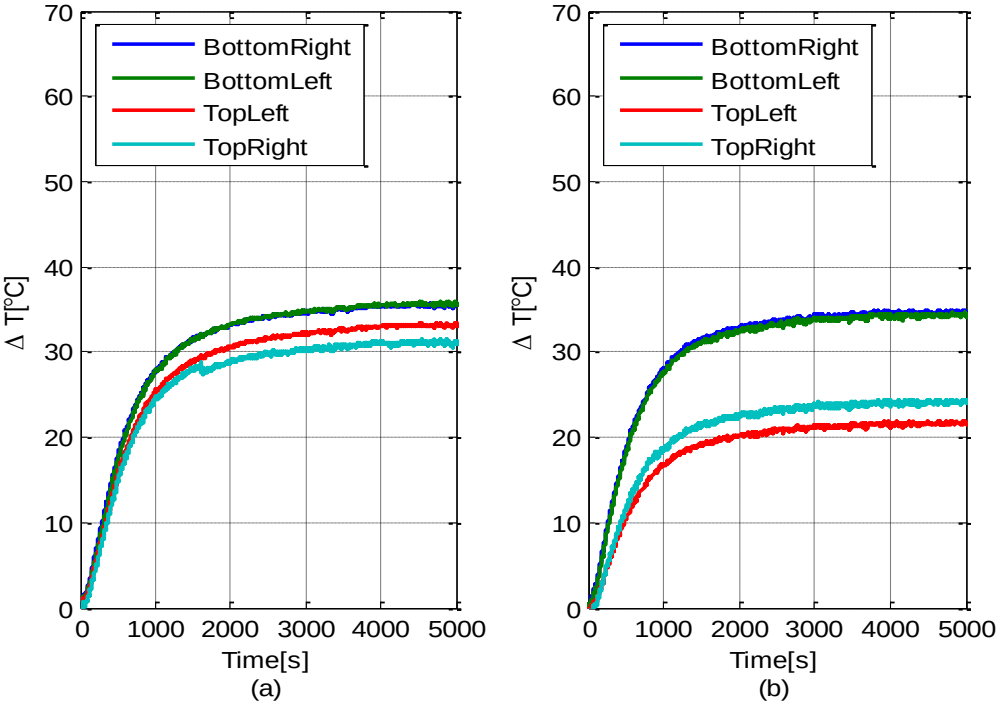

Figure 5-9 Transient behavior of Bearing sleeve temperature distribution at 37SLPM (=609pa pressure difference along axial direction) (a) Radial cooling (b) Axial cooling

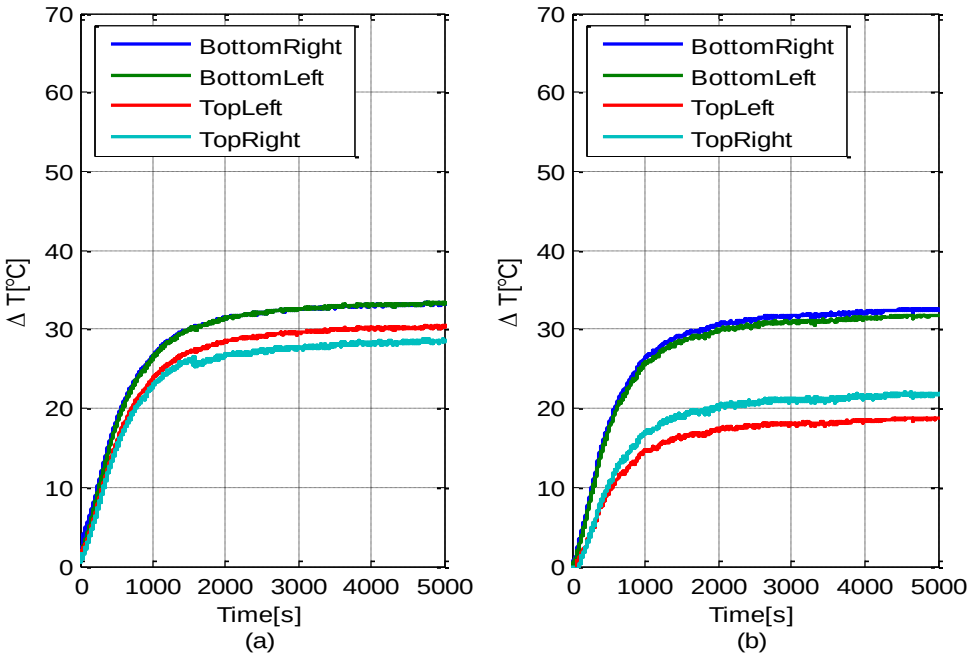

Figure 5-10 Transient behavior of Bearing sleeve temperature distribution at 46SLPM (=782pa pressure difference along axial direction) (a) Radial cooling (b) Axial cooling

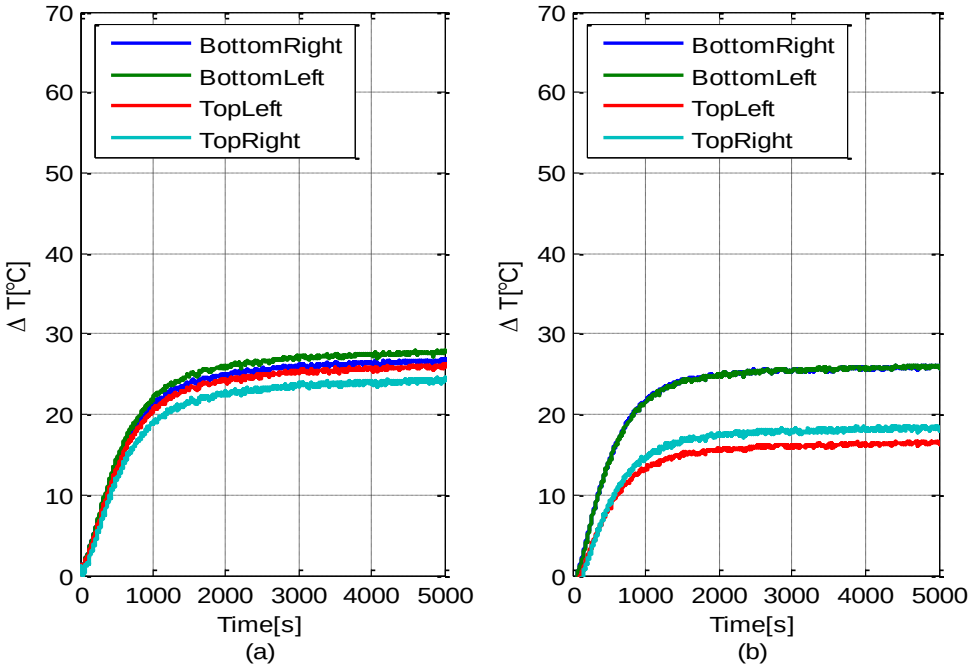

Figure 5-11 Transient behavior of Bearing sleeve temperature distribution at 57SLPM (=998pa pressure difference along axial direction) (a) Radial cooling (b) Axial cooling

5.4.2 Plenum Air Temperature Comparison

As shown in Figure 4-4, thermocouples were placed in both the cooling jacket for the temperature measurement at plenum 1 and plenum 2.

It should be noted from the Figure 5-12 through Figure 5-15 that for radial cooling both plenums air temperature are similar. Ideally, both the plenums temperature for radial cooling should have same temperature. These plenums temperature rise are due to similar effect such as convective heat transfer from rotor surface exposed and side leakage of air film to the plenums. However, the discrepancy is observed in the result which could be due to the difference is seal clearance and local rubbing.

For axial cooling case, there was much larger temperature difference between plenum 1 and plenum 2. Even if the supplied cooling air temperature at Plenum 1 is at 20^{o}C, convective heat transfer from the rotor surface and air film increases the plenum 1 air temperature before it even enters the bump channels. The air that passes through bump channels, taking the heat from bearing, is ejected to plenum 2 which results is much higher temperature at plenum 2.Also heat transfer from rotor surface exposed to the plenum facilitates increase in temperature in plenum 2.

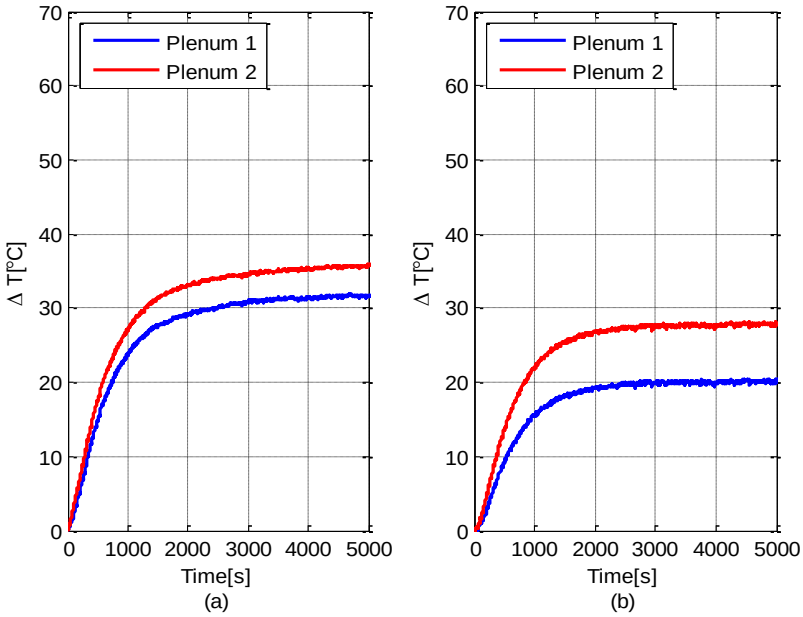

Figure 5-12 Transient behavior of Plenum temperature at 28SLPM (=444pa pressure difference along axial direction) (a) Radial cooling (b) Axial cooling

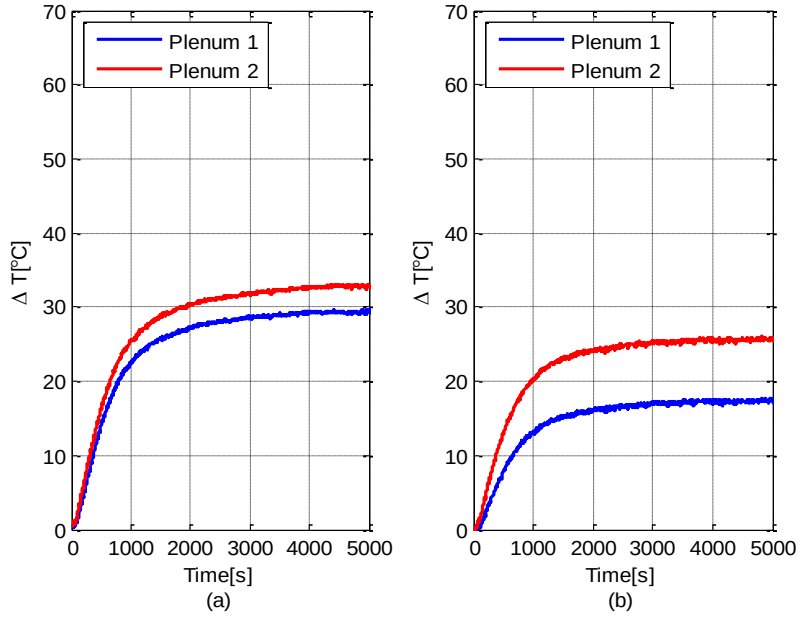

Figure 5-13 Transient behavior of Plenum temperature at 37SLPM (=609pa pressure difference along axial direction) (a) Radial cooling (b) Axial cooling

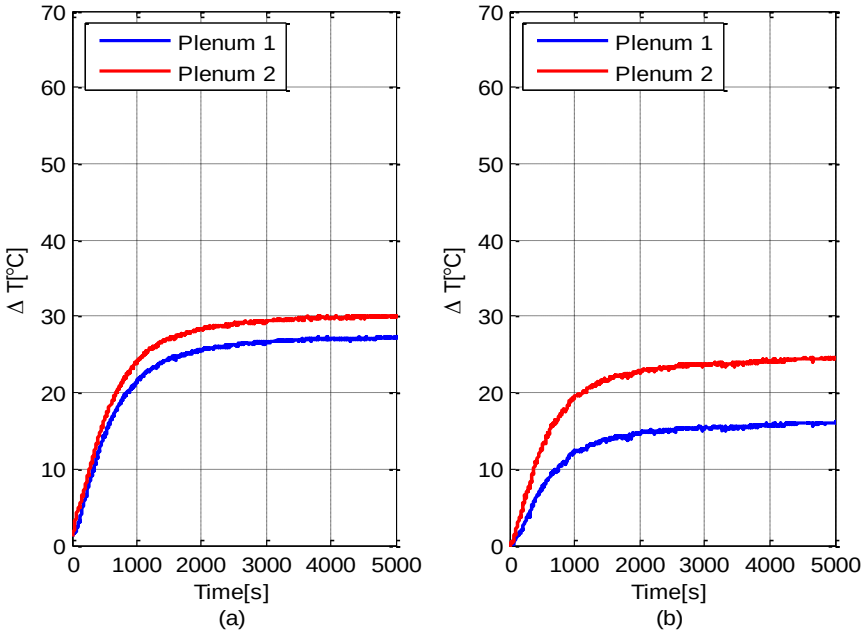

Figure 5-14 Transient behavior of Plenum temperature at 46SLPM (=782pa pressure difference along axial direction) (a) Radial cooling (b) Axial cooling

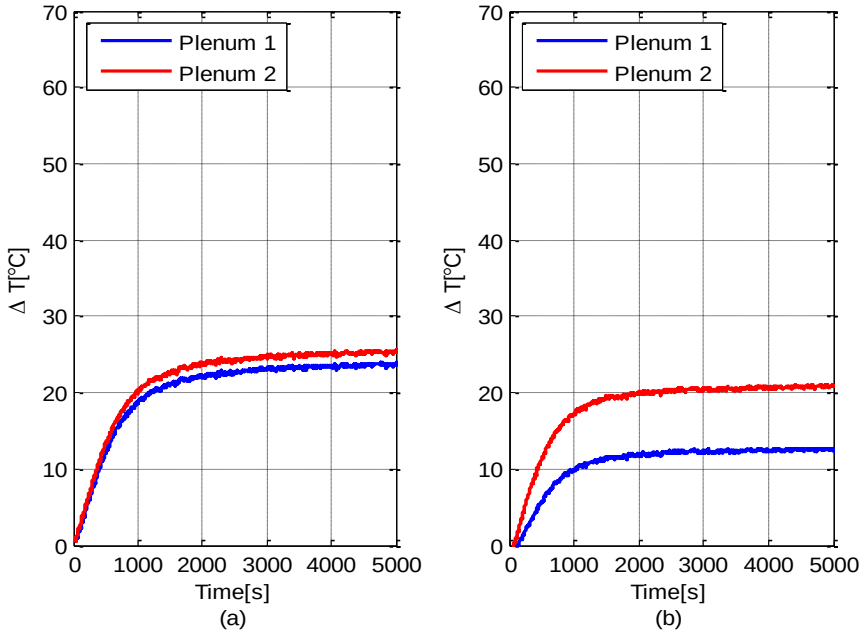

Figure 5-15 Transient behavior of Plenum temperature at 57SLPM (=1000pa pressure difference along axial direction) (a) Radial cooling (b) Axial cooling

5.4.3 Bearing Holder Temperature Comparison

Figure 5-16 shows outer surface temperature of the bearing holder with various flow rates for both radial and axial cooling methods. It can be observed from figure below that axial cooling is more effective in controlling the holder temperature compared to radial cooling. This could be the result of cooling effect due to air flowing through the bump channels. In case of radial cooling the hot air is recirculated inside the bearing before it escapes to the plenums, raising the temperature of the holder. Bearing holder temperature as shown below is lowest among all other bearing components because it is exposed to ambient environment.

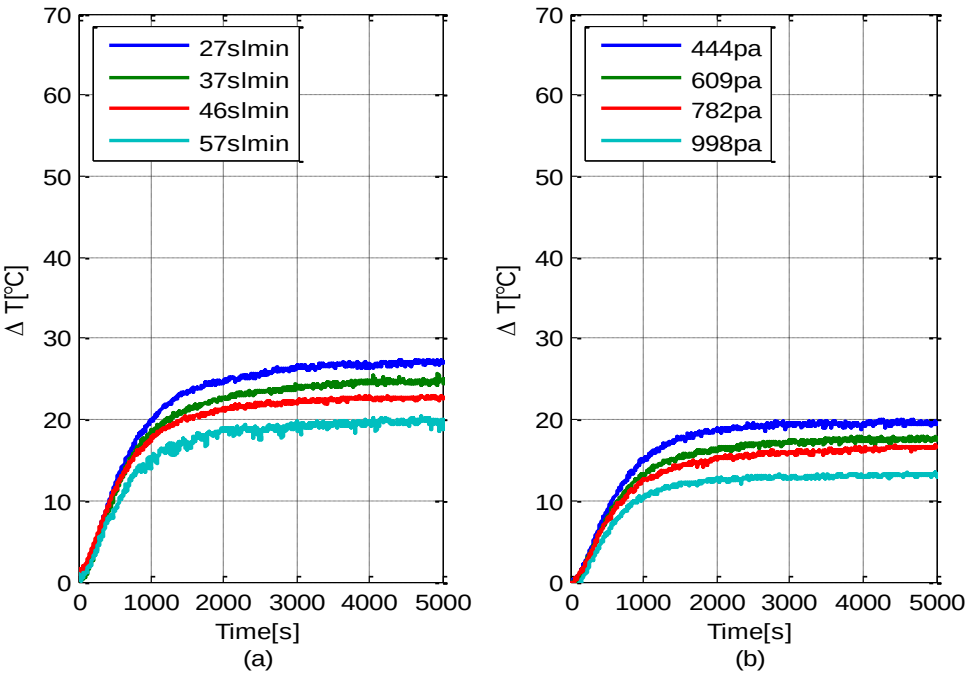

Figure 5-16 Transient behavior of Bearing holder temperature at different mass flow rates with (a)Radial cooling (b) Axial cooling

5.4.4 Ball bearing housing temperature comparison

From Figure 5-17 and Figure 5-18, it can be seen that various mass flow rate were applied in sets of experiment conducted yet there was no effect on the ball bearing housing temperature. The steady state temperature of the ball bearing is same regardless of the mass flow rate and the cooling methods used. This was as predicted and was considered validation of fact, experiments were conducted under the similar bearing parameters and operating conditions such as bearing loading, rotor speeds, and so on.

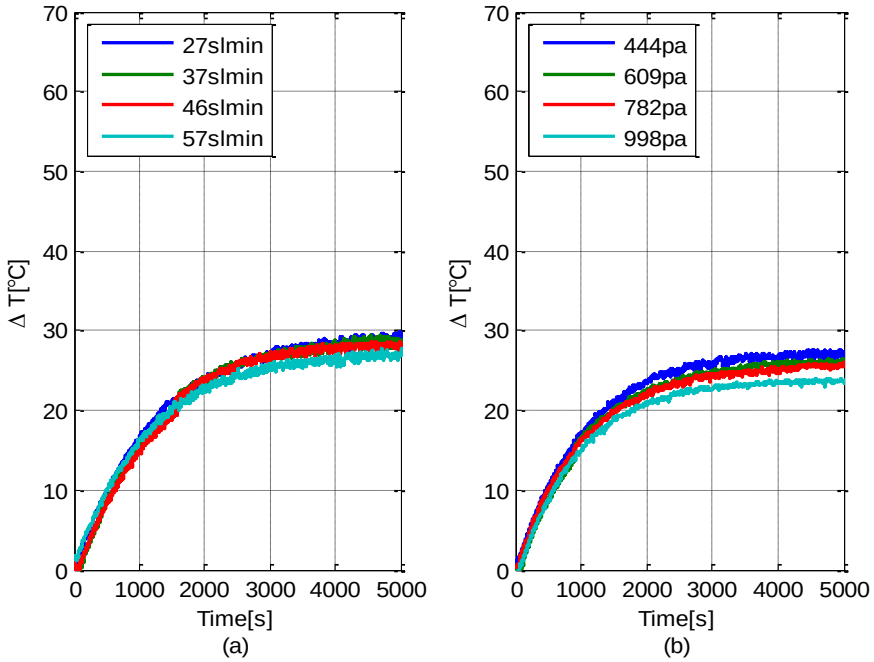

Figure 5-17 Transient behavior of Out-ward ball bearing temperature at different flow rates (a) Radial cooling (b) Axial cooling

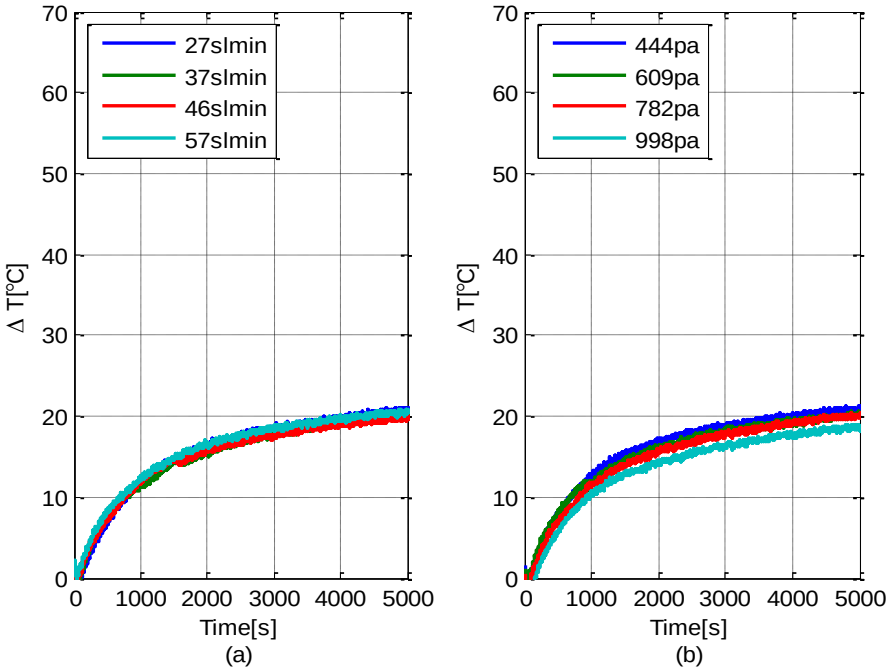

Figure 5-18 Transient behavior of In-ward ball bearing temperature at different flow rates (a) Radial cooling (b) Axial cooling

All of the figures above showing transient behavior are summarized in Figure 5-19 through Figure 5-22.It can be observed from Figure 5-19 that the cooling effectiveness increases with increase in radial injection speed of the cooling air. Similar trend is followed by Figure 5-20 for axial cooling, however it should be noted that thermal gradient is higher for the axial cooling compared to the radial injection method. Figure 5-21 and Figure 5-22 shows the temperature measurement of two plenums with different flow rates and pressure difference in these plenums respectively. As projected the plenums temperature for radial cooling method are similar for particular flow rate and that for axial cooling vary.

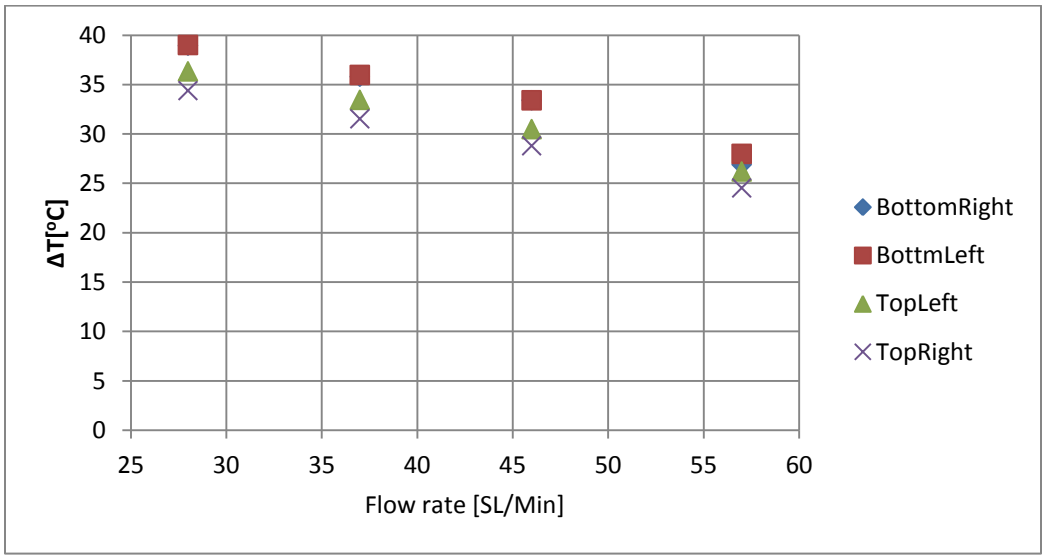

Figure 5-19 Temperature distribution in bearing sleeve with various flow rates using radial cooling method

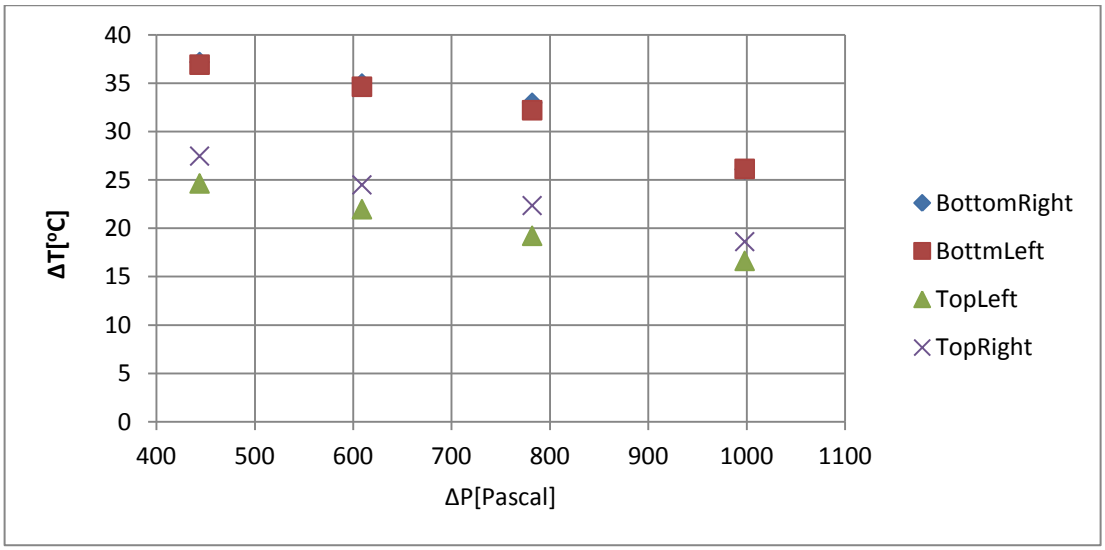

Figure 5-20 Temperature distribution in bearing sleeve with various flow rates using axial cooling method

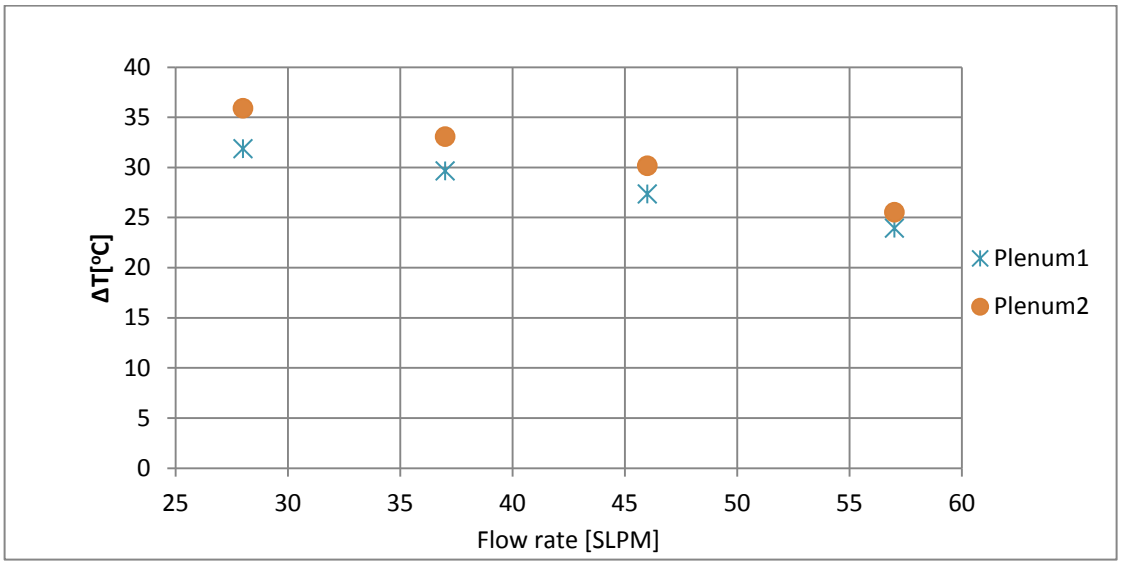

Figure 5-21 Temperature measured in two plenums with various flow rates using radial cooling method

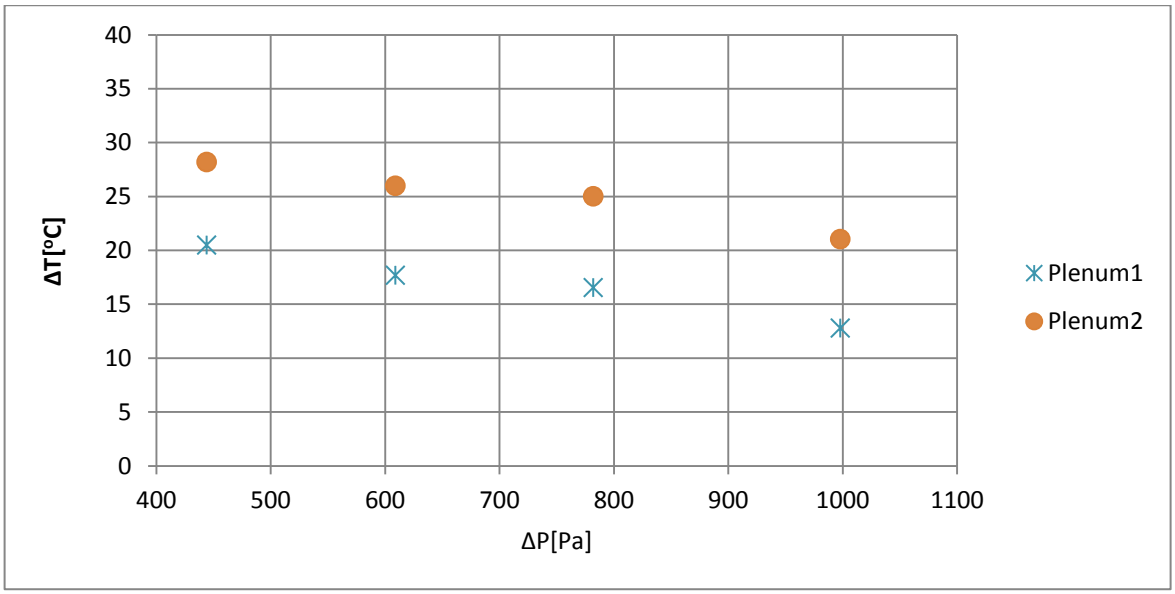

Figure 5-22 Temperature measured in two plenums with various flow rates using axial cooling method

Rotor temperature were measured at two points,shaftin and shaftout as shown in Figure 3-4.It was observed that the direct impingement of air had better effect on maintaining the thermal gradient in axial direction of the shaft compared to axial cooling(see Figure 5-23).

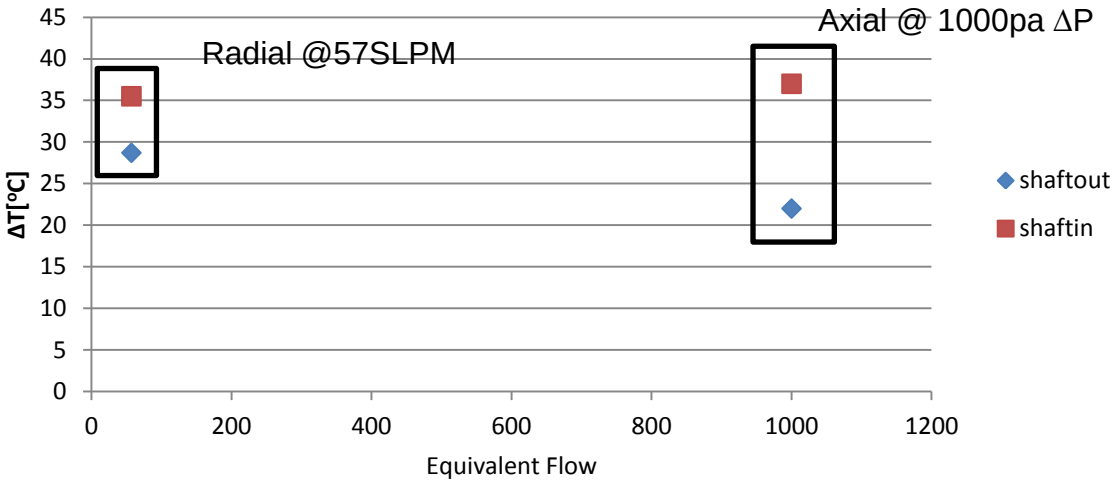

Figure 5-23 Rotor temperature at 30krpm with radial and axial cooling

CHAPTER 6

CONCLUSION AND FUTURE WORK

In terms of cooling mechanism both the methods were effective in lowering the bearing overall temperature and the effectiveness in both methods was proportional to the flow rates. However, the effectiveness of axial cooling slightly exceeded that of radial cooling in controlling the mean temperature especially for the bearing sleeve which can be credited to the proper use of bump channel during axial cooling method. But the results for thermal gradient in the bearing sleeve along circumferential direction and also thermal gradient of the shaft along axial direction proved radial injection to be better. The smaller thermal gradient value of the radial injection is attributed to the direct cooling effect of the shaft by impinging jets. While the axial cooling has an effect on only the bearing, the radial injection has a cooling effect on both the bearing sleeve and shaft.

The future work may include the modification of current journal shaft design. As shown in Figure 6-1, bump foil is press fitted between the journal and intermediate journal shaft .This design would isolate the journal shaft from the rest of the test rig. Also the bump foil channels would serve as the heat exchanger reducing the thermal growth of the journal shaft.

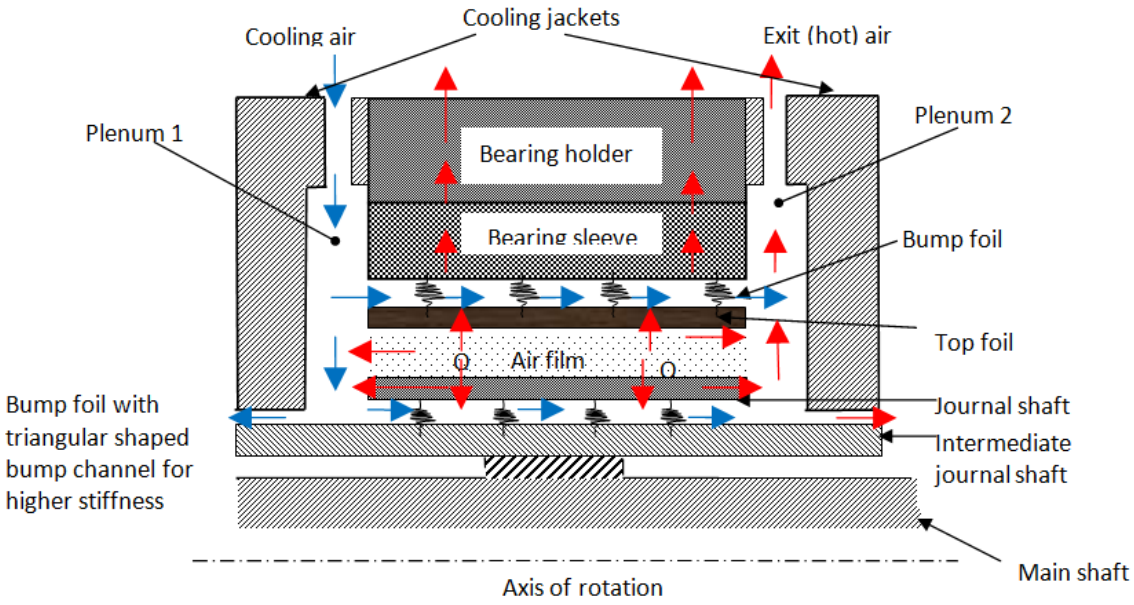

Figure 6-1 Journal shaft axial cooling design

APPENDIX A

TEST RIG SETUP, TOP FOIL FORMATION PROCESS AND PROGRAMMABLE FURNACE

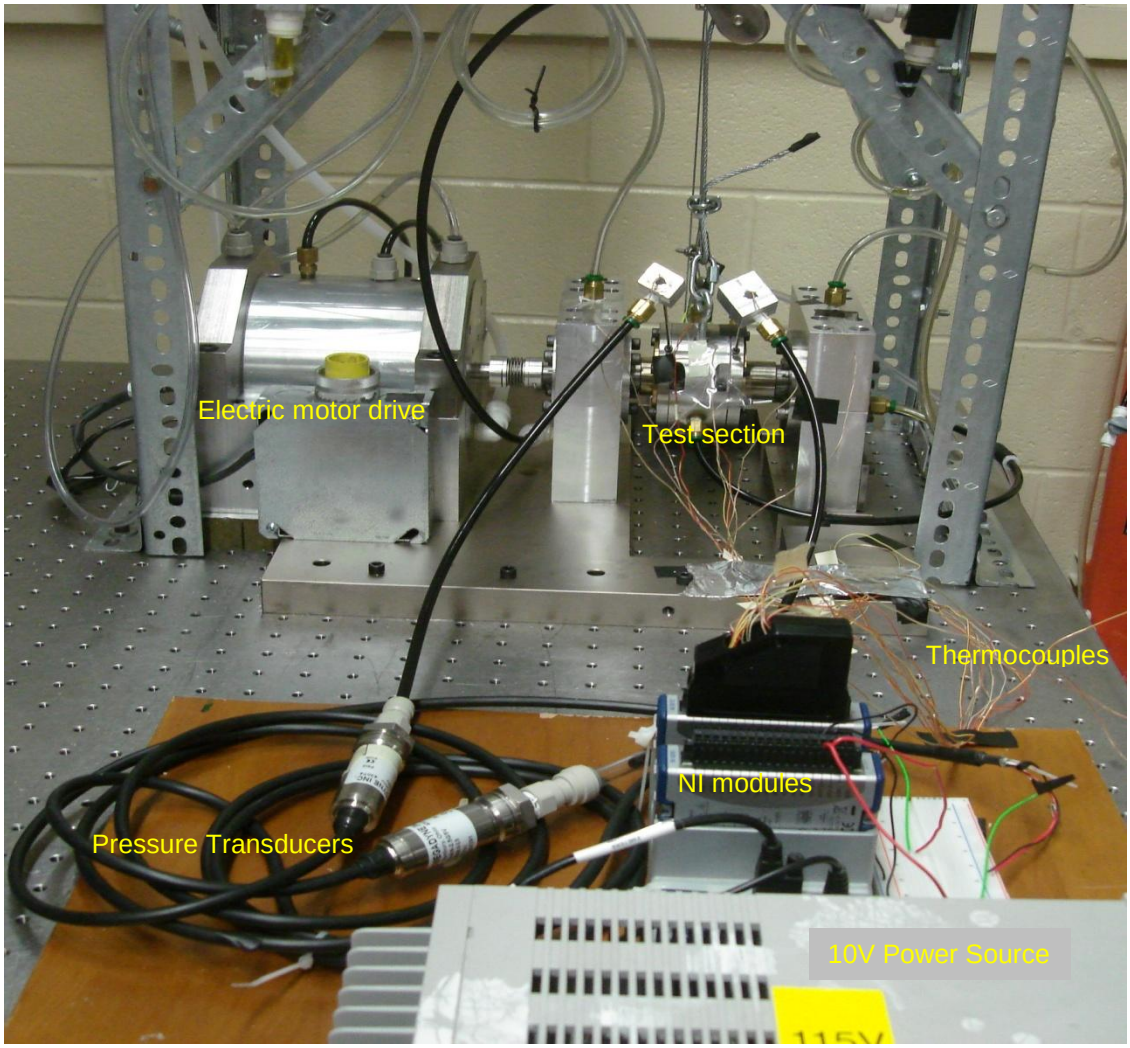

Figure A-1 Test Rig Setup with data collection instrumentation

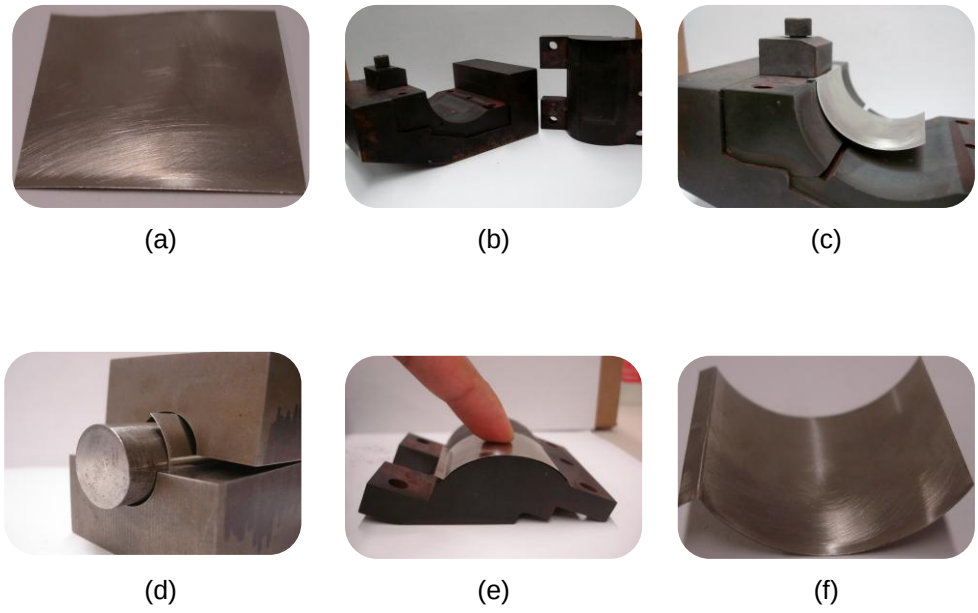

Figure A-2 Description of the steps to form top foil for AFB (a) Blank sheet (b) Jig to form lip (c) Formed lip(d) Jig to form curvature (e) Top foil following bearing sleeve curvature (f) Formed top foil with required shape.

REFERENCES

[1] Radil, K., DellaCorte, C., and Zeszotek, M., 2007, "Thermal Management Techniques for Oil-Free Turbomachinery Systems," STLE Tribology Transactions**, 63**(10), pp. 319-327.

[2] Radil, K., and Batcho, Z., 2011, "Air Injection as a Thermal Management Technique for Radial Foil Air Bearings," Tribology Transactions**, 54**(4), pp. 666-673.

[3] Lee, D., and Kim, D., 2010, "Thermo-Hydrodynamic Analyses of Bump Air Foil Bearings with Detailed Thermal Model of Foil Structures and Rotor," ASME Journal of Tribology**, 132**(2), pp. 021704 (12 pages).

[4] Kim, D., Ki, J., Kim, Y., and Ahn, K., 2011, "Extended Three-Dimensional Thermo-Hydrodynamic Model of Radial Foil Bearing: Case Studies on Thermal Behaviors and Dynamic Characteristics in a Turbine Simulator," Accepted to ASME Journal of Engineering for Gas Turbines and Power.

[5] Radil, K., and Zeszotek, M., 2004, "An Experimental Investigation into the Temperature Profile of a Compliant Foil Air Bearing," STLE Tribology Transactions**, 47**(4), pp. 470-479.

[6] Lee, D., Kim, D., and Sadashiva, R. P., 2011, "Transient Thermal Behavior of Preloaded Three-Pad Foil Bearings: Modeling and Experiments," Journal of Tribology**, 133**(2), pp. 021703.

[7] Radil, K., Howard, S., and Dykas, B., 2002, "The Role of Radial Clearance on the Performance of Foil Air Bearings," STLE Tribology Transaction**, 45**(4), pp. 485-490.

[8] Salei, M., Swanson, E., and Heshmat, H., 2001, "Thermal Features of Compliant Foil Bearings – Theory and Experiments," ASME Journal of Tribology**, 123**(3), pp. 566-571.

[9] Song, J., and Kim, D., 2007, "Foil Gas Bearing with Compression Springs: Analyses and Experiments," ASME Journal of Tribology**, 129**(3), pp. 628-639.

[10] Kim, D., Lee, D., Kim, Y. C., and Ahn, K. Y., 2010, "Comparison of Thermo-Hydrodynamic Characteristics of Airfoil Bearings with Different Top Foil Geometries," Proceedings of the 8th IFToMM International Conference on Rotordynamics, Seoul, Korea, September 12-15, Paper No. WeD1-4.

[11] Lee, D., Kim, D., and Sadashiva, R. P., 2011, "Transient Thermal Behavior of Preloaded Three-Pad Foil Bearings: Modeling and Experiments," ASME Journal of Tribology**, 133**(2), pp. 021703 (11 pages), doi: 10.1115/1.4003561.

[12] R. P. SADASHIVA, 2010, *EXPERIMENTAL INVESTIGATION OF THERMAL BEHAVIOUR OF AIR FOIL BEARINGS,* MS thesis, The University of Texas at Arlington.

BIOGRAPHICAL INFORMATION

Suman K. Shrestha graduated from University of Texas at Arlington in spring 2010 with Bachelor of Science degree in Mechanical Engineering. He was involved with Dr. Daejong Kim in his Microturbomachinery and Energy Systems Laboratory since he was an undergraduate student. He continued on for his M.S Degree in Mechanical Engineering. He has worked at the Microturbomachinery and Energy Systems Laboratory since 2009 and has been involved in numerous projects including feasibility study of radial injection cooling of three-pad radial air foil bearing which is the topic of this thesis.